© 2020. This manuscript version is made available under the CC-BY-NC-ND 4.0 license http://creativecommons.org/licenses/by-nc-nd/4.0/
https://doi.org/10.1016/j.scitotenv.2020.142671

Analysis and optimisation of a novel 'Almond-refinery' concept: Simultaneous production of biofuels and value-added chemicals by hydrothermal treatment of almond hulls

Javier Remón[a]*, Javier Latorre-Viu[a], Avtar S. Matharu[b], José Luis Pinilla[a], Isabel Suelves[a]
[a]Instituto de Carboquímica, CSIC. C/Miguel Luesma Castán 4, 50018 Zaragoza, Spain.
[b]Green Chemistry Centre of Excellence, University of York, Department of Chemistry, Heslington, York, YO10 5DD, UK.
*Corresponding author: jremon@icb.csic.es

Abstract:

For the first time, this work investigates the achievability of developing a biorefinery concept around almond hulls by hydrothermal treatment (HTT), thoroughly scrutinising the influence of the temperature (200-300 ºC), pressure (100-180 bar), time (20-180 min) and solid loading (5-25 wt.%). This process allowed the conversion of almond hulls into four main products: gas (2-13%), bio-oil (2-12%), aqueous (4-69%) and hydro-char (17-89%). The gas consisted of a mix of H_2, CO_2, CO and CH_4 with a LHV fluctuating from 1 to 13 MJ/m^3 STP. The bio-oil comprised a mixture of alkanes, aldehydes, ketones, phenols, furans, benzenes and nitrogen compounds with a HHV between 21 and 31 MJ/kg. The solid product resembled an energetic hydro-char material (HHV 21-31 MJ/kg), while the aqueous effluent comprised a mixture of value-added chemicals, including saccharides and small oxygenated compounds. The production of biofuels can be maximised at 256 ºC and 100 bar, using a 5 wt.% solid loading for 157 min, conditions at which 43% of the original feedstock can be converted into an elevated energy-filled bio-oil (11% yield, 30 MJ/kg), along with a high energetic hydro-char (32% yield, 29 MJ/kg). Regarding value-added chemicals, up to 10% of the almond hulls can be converted into a bio-oil with a high proportion (45%) of phenolic species at 250 ºC and 144 bar with a solid loading of 5 wt.% for 167 min. In comparison, a sugar-rich (81 C-wt.%) solution can be produced in high yield (54%), by treating a 24 wt.% suspension at 252 ºC and 180 bar for 153 min. Therefore, the versatility, novelty and intrinsic green and holistic nature of this 'almond-refinery' concept exemplify a landmark achievement in future energy and chemicals production from biomass, which might help render the complete bio-refinery for almond hulls more cost-effectively and ecologically feasible.

Keywords: almond hulls, hydrothermal treatment, biorefinery, bio-fuels, value-added chemicals

1. Introduction

The substantial increase in the request for energy and chemicals worldwide, along with the environmental concerns related to such variations, have led researches to investigate the use of feedstock alternatives to

petroleum, as well as to create innovative, carbon-neutral and more efficient procedures for manufacturing these supplies in a more sustainable manner. Within this global renewable energy picture, second (lignocellulosic) and third (algae) generations of biomass, as well as organic wastes are regarded as very promising feedstocks to obtain these commodities using a 'waste to wealth strategy' (Clark, 2019). This approach, which is usually conceptualised as a biorefinery, primarily focuses on the valorisation of unavoidable biomass residues for the production of biofuels, chemicals and materials (Attard et al., 2020; Clark, 2019). Among the different lignocellulosic wastes worldwide, almond hulls, produced as a by-product in the almond processing industry, are an attractive and almost unexploited candidate for the production of these commodities. Almond hull, also known as almond green shell cover, is the outer covering of the almond kernel and shell and accounts for more than half of the total almond weight (Esfahlan et al., 2010). It contains insoluble fibre (mainly comprising cellulose, hemicellulose and pectin), together with tannin-like poly-phenolic compounds, lignin and ash (Esfahlan et al., 2010). It must be born in mind that almonds production has increased dramatically over the past few years, e.g. worldwide production has raised from around 0.7 millions of tons in 2007 to 1.5 millions of tons in 2019 (April 2020a; April 2020b). Therefore, it is necessary to develop novel strategies for the management of this by-product of the almond industry, since the sustainable valorisation of almond hulls might be an up-and-coming option not only to deal with this residue but also to decrease our current dependence to fossil fuels.

Notwithstanding almond hulls renewable nature and global availability, work addressing the valorisation of this material is very scarce. In the past, almond hulls were seen as a potential source of foods, foods additives and pharmaceuticals, due to the possibility of recovering valuable compounds for these industries such as chlorogenic, crypto chlorogenic and neochlorogenic acids, saccharides (sucrose, glucose, fructose), sugar alcohols (inositol and sorbitol) and sterols (stigmasterol and b-sitosterol). (Esfahlan et al., 2010; Sfahlan et al., 2009). However, they were primarily used as supplemental livestock feed. Few recent studies addressed the valorisation of almond hulls; however, they mostly focused on the extraction of several compounds such as sugars, nutraceuticals and/or phenolic derivatives, instead of developing a process for the complete valorisation of the whole material. Regarding extraction of phenols, Pinelo et al. (2004) used ethanol, methanol and water to extract phenolic compounds from almond hulls,

reporting a good antioxidant activity (58% oxidation inhibition measured by DPPH radical-scavenging assay). In this line, Sfahlan et al. (2009) compared the antioxidant and antiradical activity of hulls obtained from different almonds varieties, including *Amygdalus Communis L.* and *Communis L.* Genotypes, using methanol (3g solid/50 mL solvent) at 80 ºC for 30 min. Kahlaoui et al. (2019) used an ultrasound-assisted extraction process to recover phenols from almond hulls of four Tunisian and three Italian almond varieties using ethanol as a solvent. Concerning the production of carbohydrates, Offeman et al. (2015) conducted hot water extraction experiments to recover the carbohydrate content of hulls obtained from the almond *Prunus Dulcis*, examining the effects of the temperature and solid particle size. They found that 58% of the dry matter content of the hulls was soluble in warm water. These extracts were primarily made up of fermentable sugars (glucose, fructose, sucrose) and sugar alcohols (inositol and sorbitol). In another work, these authors compared the amount of sugar produced from *Nonpareil, Monterey, Butte, Padre, Carmel, and Fritz* almonds, by hot water extraction (Offeman et al., 2014). As regards to bio-materials and energy applications, Ferrandez-Villena et al. (2019) used almond hulls to manufacturing renewable particleboards, analysing the influence of the hull initial particle size. Using particle sizes lower than 0.25 mm, it was possible to achieve a bio-material with high strength, in terms of moduli of rupture and elasticity and internal bonding strength. González et al. (2005) analysed the combustion of tree pruning and almonds shell and hull, reporting efficiencies of 88%, 85% and 79%, respectively.

Even though these works provide useful insights into the valorisation of almonds hulls via the recovery of some of their constituents, it is still necessary to develop novel strategies to achieve a complete and more sustainable valorisation of the whole material, rather than recovering only several compounds, which leaves a spent solid as a by-product, which may need further management. As such, a very appealing option that has not been addressed before is the concurrent production of biofuels and value-added platform chemicals by hydrothermal treatment (HTT), including hydrothermal liquefaction (HTL) and carbonisation (HTC). This thermochemical route could be effectively used to establish an environmentally-friendly bio-refinery model for almond hulls; i.e., a novel ‘almond-refinery’ approach. This new approach not only represents a substantial improvement for the implementation of novel, more integrated and holistic biorefinery procedures but also it helps decrease the hazardous generation of by-

93 products. HTT is a relatively new thermochemical process which allows biomass transformation into
94 gaseous, liquid and solid products, using water (one of the greenest solvents) at subcritical conditions
95 (temperatures of 150-400 ºC and pressures between 5-25 MPa) as the reaction medium (Arturi et al.,
96 2016; Dimitriadis and Bezergianni, 2017; Elliott et al., 2015a; Elliott et al., 2015b; Gollakota et al., 2018;
97 Kumar et al., 2018; Toor et al., 2011).
98
99 Besides, it is essential to note that during HTT, the water is the liquid phase and it is not necessary to dry
100 the raw material; both aspects remarkably contributing to improving the energetic profitability of future
101 bio-refineries. These intrinsic features are of especial interest for the upgrading of feedstocks with high
102 moisture content, such as almond hulls. Also, it must be borne in mind that HTT also owns several
103 inherent advantages for biofuels production if compared to other thermochemical processes, such as fast
104 pyrolysis and/or gasification. These include using much lower temperatures along with the better
105 physicochemical properties of the products obtained, i.e., the bio-oils and chars produced via HTT of
106 lignocellulosic biomass have lower oxygen contents and, therefore, higher calorific values than those
107 obtained by fast pyrolysis (Dimitriadis and Bezergianni, 2017; Elliott et al., 2015a; Kumar et al., 2018;
108 Toor et al., 2011). Although there is quite a substantial work covering the potential applicability of this
109 valorisation process for the conversion of biomass into bio-oil (bio-crude) (Gollakota et al., 2018) and/or
110 hydro-char (Saqib et al., 2019), to the best of our knowledge, HTT has never been used for the valorisation
111 of almond hulls. Besides, this process has commonly being directed towards the production of one
112 specific product from lignocellulosic biomass; i.e., bio-oil or hydro-char. As such, works addressing the
113 effect of process conditions on the distribution and properties of the products (bio-oil, hydro-char,
114 aqueous and gas) are scarce. Consequently, this work not only provides new information on the
115 management and valorisation of almond hulls but also on the HTT of lignocellulosic biomass.
116
117 Herein, this paper explores, for the first time, the valorisation of almond hulls by HTT, thoroughly
118 investigating the impact on the process of the temperature (200-300 ºC), total pressure (100-180 bar),
119 reaction time (20-180 min) and solid/water ratio (5-25 wt.%). This includes the full effects of the process
120 parameters on the yields to products (gas, bio-oil, aqueous fraction and hydro-char) and key
121 physicochemical properties of these fractions, such as elemental and chemical compositions and calorific

values. Given that HTT has never yet been reported for the treatment of almond hulls and/or any almond by-products, and the thorough process analysis conducted, prove that this investigation is a new and essential step forward in this field. Thus, this work contributes not only towards the development of a green and energy-efficient bio-refinery concept around almond hulls, but also it makes a landmark accomplishment to create a whole bio-refinery for lignocellulosic wastes more cost-effectively and ecologically feasible.

2. Experimental

2.1 Hydrothermal treatment

The HTT tests were run in a 100 mL batch, pressurised autoclave (Parker Autoclave Engineers) made of stainless steel. An external heating jacket was used to heat the reactor vessel, while a thermocouple, located inside the reactor vessel and connected to a PID control, was employed to monitor and control the temperature. A stirrer bar, controlled by a magnetic rotor (Magnedrive), was used to homogenise the reaction mixture during the reaction, while a coiled tube and a baffle aided to create a turbulent regime. More information about the experimental set-up can be found elsewhere (Ochoa et al., 2018; Ochoa et al., 2019; Remón et al., 2019b). For each experiment, 50 mL of deionised water was loaded in the reactor together with different amounts of almond hulls according to the experimental design used in this work. Then, the reactor was pressurised with N_2 using an internal calibration to achieve reaction conditions. After each run, the reactor was quenched to decrease the temperature as quickly as possible. Once chilled, at a temperature between 50 and 60 ºC, a gas sample was collected using a gas bag for the analysis of the gas phase. Then, the reactor was opened, and the liquid and solid products were recovered. The reactor vessel and the stirrer were rinsed with chloroform, and both fractions were subjected to a solid-liquid extraction in a separation funnel. The solid (hydro-char) was dried overnight at 105 ºC, weighed and stored for further analysis. The liquid phase, comprising a bio-oil and an aqueous liquid product, was subjected to a bio-oil recovery process using chloroform ($CHCl_3$) and ethyl acetate (EtOAc) as the solvents, following the methodology reported by Ren et al. (2017). The aqueous product was weighed and stored for further analysis. Then, the bio-oil recovered in the organic extraction mixture ($CHCl_3$ and EtOAc) was subjected to a two-step separation procedure. Firstly, a rotary evaporator was used to remove

$CHCl_3$ and EtOAc substantially; secondly, a stream of pure nitrogen gas was used to completely evaporate the remaining solvents and recover the bio-oil, which was weighed and stored for further analysis.

2.2 Response variables and analytical methods

Different response variables were used to elucidate the effects of the operating conditions on the process. These include the gas, bio-oil, aqueous fraction and solid (hydro-char) yields along with their most representative fuel and chemical properties.

Table 1. Response variables and methods

Product	Response variable	Method
Gas	$\text{Gas yield (\%)} = \frac{\text{mass of gas (g)}}{\text{mass of biomass (g)}} 100$	Gas Chromatography
	$\text{Composition (vol.\%)} = \frac{\text{mol of each gas}}{\text{total mol of gas}} 100$	Gas Chromatography
	LHV (MJ/m^3 STP) = 0.1079 H_2 (vol.%) + 0.1263 CO (vol.%) + 0.3581 CH_4 (vol.%)	Estimated
Bio-oil	$\text{Bio} - \text{oil yield (\%)} = \frac{\text{bio} - \text{oil (g)}}{\text{mass of biomass (g)}} 100$	Gravimetric
	$\text{C, H, O, N, S (wt.\%)} = \frac{\text{mass of C, H, O, N (g)}}{\text{mass of bio} - \text{oil (g)}} 100$	Elemental Analysis
	HHV (MJ/kg) = 0.3491 C (wt.%) + 1.1783 H (wt.%) – 0.1034 O (wt.%) – 0.015 N (wt.%) + 0.1005 S (wt.%). (Channiwala and Parikh, 2002)	Estimated
	$\text{Composition (Area \%)} = \frac{Area\ of\ each\ compound}{\text{Total area of compounds}} 100$	GC/MS
Liquid (aqueous)	$\text{Liquid yield (\%)} = \frac{\text{liquid compounds (g)}}{\text{mass of biomass (g)}} 100$ $= 100 - (\text{Gas yield} + \text{Bio} - \text{oil yield Solid yield})$	Balance
	$\text{Composition (C} - \text{wt.\%)} = \frac{\sum \text{mass of C of each compound (g)}}{\text{total mass of C in solution (g)}} 100$	HPLC
	$\text{C, H, O (wt.\%)} = \frac{\text{mass of C, H, O, N (g)}}{\text{mass of liquid(g)}} 100$	Elemental Analysis
Solid	$\text{Solid yield (\%)} = \frac{\text{mass of solid (g)}}{\text{mass of biomass (g)}} 100$	Gravimetric
	HHV (MJ/kg) = 0.3491 C (wt.%) + 1.1783 H (wt.%) – 0.1034 O (wt.%) – 0.015 N (wt.%) + 0.1005 S (wt.%). (Channiwala and Parikh, 2002)	Estimated
	$\text{C, H, O, N (wt.\%)} = \frac{\text{mass of C, H, O, N (g)}}{\text{mass of solid (g)}} 100$	Elemental Analysis
Energy Efficiency	$\text{E(\%)} = \frac{Gas\ yield \cdot LHV + \quad io - oil\ yield \cdot HHV + \quad io - char\ yield \cdot HHV}{\text{HHV almond hulls}} 100$	Calculated

Table 1 recaps these response variables and summarises the methodologies employed for calculation. These comprise gas chromatography to determine the composition of the gas phase, elemental analysis, calorific value and gas chromatography for the study of the bio-oil, High-Performance Liquid Chromatography and elemental analysis to determine the chemical composition of the aqueous product on a C basis and elemental analysis and heating value for the characterisation of the hydro-char. Specifically, a micro gas chromatograph (micro GC Varian CP4900) equipped with two packed columns (Molecular sieve and Porapack), coupled to a TCD detector was used for the analysis of the gas phase, using standards of H_2, N_2, CO, CO_2 and CH_4 for identification and quantification. The gas yield was

168 determined as the total amounts of H_2, CO, CO_2 and CH_4 in the mixture. An ideal gas behaviour, at the
169 temperature and pressure at which the gas sample gas collected, was assumed for this calculation. The
170 LHV of the gas was calculated as the pondered heat of combustion of each gas taking into account the
171 gas mixture volumetric composition. For the gas chromatography-mass spectroscopy (GC-MS) analyses,
172 an aliquot of each bio-oil produced was dissolved in a $CHCl_3/CH_3OH$ (2:1 vol.) solution. Then, the
173 samples were analysed in an Agilent 7890 GC-system. An Agilent 1260 Infinity HPLC was used for the
174 characterisation of the liquid effluent. The characteristics can be found in the supplementary information.
175 The oligosaccharides concentration was calculated as the difference between the amount of C determined
176 by elemental analysis and the amount of C measured by HPLC. More detailed information about the
177 experimental analysis procedure and apparatus can be found elsewhere (Remón et al., 2018b). Elemental
178 analyses were conducted using a Carlo Erba EA1108 Elemental Analyser. The empirical formula
179 developed by Channiwala and Parikh (2002) was employed to determine the HHV of the bio-oil and
180 hydro-char.
181
182 **2.3 Experimental design and statistical analyses**
183 The influences on the hydrothermal treatment of the reaction temperature, total pressure, time and
184 solid/water ratio were analysed experimentally through a 2 level 4 factor (2^4) Box-Wilson Central
185 Composite Face Centred (CCF, α: ±1) design. This design comprises 2^4 (16) experiments for the analysis
186 of linear effects and interactions, along with 4 centre points, i.e., repeats at intermediate conditions to
187 calculate the error variance, and 8 axial experiments to determine the possible influence of quadratic
188 effects and quadratic interactions. The results obtained during the HTT experiments were statistically
189 analysed with a 95% confidence ANOVA and the cause-effect Pareto test. For these analyses, the
190 intervals of variations were standardised to vary between -1 and +1, which allowed all the factors to
191 change within the same interval. Therefore, the relative importance of each operating variable can be
192 easily gathered. The ANOVA permitted the selection of the processing variables and interactions between
193 variables with a significant impact on the HTT results. At the same time, the cause-effect Pareto test was
194 employed to determine the comparative influence of these factors on the experimental results. In the
195 ANOVA analysis, the least significant difference (LSD) bars were built up by the design, model,
196 confidence level and unexplained variation with a confidence level of 95% (p-value 0.05). To describe

graphically and discuss the effects of the processing conditions and interactions between them, their variations were graphically represented in the interaction plots, making use of the formulae obtained in the ANOVA analysis of the 28 experiments performed. Besides, the figures include some experimental data points, when possible, to show the lack of fit is not significant. This procedure permits an exhaustive analysis of the process.

2.4 Almond hulls characterisation

Almond hulls were collected from Marcona type almonds harvested in Ricla, Zaragoza, Spain (41º 30' 20.88" N, 1º 24' 16.847"' W). Before characterisation, almond hulls were dried overnight in an oven at 60 ºC to prevent their degradation and decomposition during the experimentation period. Subsequently, they were chopped using a knife mill and sieved to a particle size between 100-200 μm. Afterwards, the dried almond hulls were characterised using several techniques to determine their structural composition and physicochemical properties. Proximate and ultimate analyses were completed following standardised methodologies (ISO-18134:2016, ISO-18122:2016 and ISO-18123:2016). Fibre characterisation, in terms of cellulose, hemicellulose and lignin, was determined following the chemical titration methodology developed by Hu et al. (2014), with the protein content being calculated with the quantity of N determined by elemental analysis (Meneses et al., 2013). Elemental analyses were done in a Carlo Erba EA1108 Elemental Analyser.

3. Results and discussion

3.1 Almond hulls characterisation results

The characterisation results of the stabilised almond hulls are summarised in Table 2. Very similar physicochemical properties to those reported by Aktas et al. (2015) and González et al. (2005) are observed for the almond hulls used in this work.

Table 2. Almond hulls characterisation

Proximate analysis (wt.%)	
Moisture	6.72 ±2.87
Ash	11.80±0.37
Volatiles	62.72±1.93
Fixed carbon	18.77±0.57
Fibre analysis (wt.%)	
Cellulose	12.60±0.77
Hemicellulose	19.40±1.17
Lignin	25.10±2.47
Proteins	7.81±0.23
Ash	11.80±0.87
Others	16.57±1.27
Ash Composition (wt.%)	
Al	0.36
Ca	6.70
Fe	0.24
K	84.76
Mg	3.61
Na	0.22
P	2.89
Si	1.21
Elemental analysis (wt.%)	
C	44.23±1.38
H	4.65±0.21
N	1.25±0.07
O[a]	49.88±1.52
HHV (MJ/kg)	15.74±0.50

[a] Oxygen was calculated by difference.

3.2 Effect of the operating conditions on the HTT of almond hulls

The detailed experimental reaction conditions employed for the tests together with the HTT results, including the yields to gas, bio-oil, aqueous fraction and solid (hydro-char), as well as key properties of these products, are included as supplementary information in Table S1. These comprise the chemical composition and Lower Heating Value (LHV) of the gas, the chemical and elemental compositions and Higher Heating Value (HHV) of the bio-oil, the chemical composition of aqueous product as well as the elemental and HHV of the bio-char. The full effects of the operating conditions on the experimental results according to the ANOVA and cause-effect Pareto principle analyses considering the 28 runs conducted are summarised in Table S2.

3.2.1 Overall products distribution: gas, bio-oil, aqueous fraction and solid yields

The HTT of almond hulls leads to the formation of four main products: gas (2-13%), bio-oil (2-12%), aqueous fraction (4-69%) and hydro-char (17-89%). The hydrothermal decomposition of biomass includes three main steps: i.) the formation of unstable species by a first biomass depolymerisation; ii.) the subsequent disintegration of these species by cleavage, dehydration, decarboxylation and deamination, which results in the creation of reactive fragments that can advance to bio-oil, liquid products and/or gas formation and iii.) the recombination and/or repolymerisation of these reactive

fragments, leading to the establishment of more bio-oil and/or resulting in carbonaceous residues, e.g. hydro-char (Gollakota et al., 2018). Given this, Figure 1 shows a schematic pathway addressing the formation of gas, bio-oil, aqueous products and hydro-char from the HTT almond hulls.

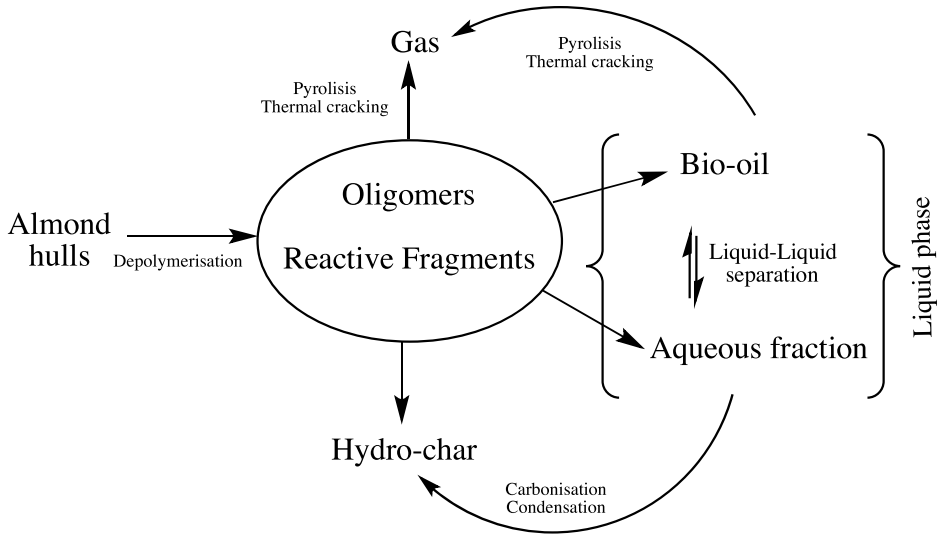

Figure 1. Schematic pathway showing the transformation of almond hulls into different products

The complete influence of the conditions determined by the cause-effect Pareto test (Table S2) is included as supplementary information. The detailed influences of these variables and interactions on the global reaction products distribution are graphically summarised in Figures 2 and 3. In particular, Figure 2 shows the effects of the temperature at the lowest and the highest (100 and 180 bar) pressures used in this work for short and long reaction times (20 and 180 min) using a solid loading of 5 wt.%. These effects are plot in Figure 3 for a solid loading of 25 wt.%. The outcomes of the temperature, pressure and reaction time on the overall distribution of reaction products depend on the solid/water ratio. For a diluted suspension (5 wt.%), the influence of the temperature depends on the pressure and reaction time (Figure 2). For a short reaction time (20 min), two different developments are observed controlled by the pressure. At low pressure (100 bar), the gas yield is low (5-7%) irrespective of the temperature. Under such pressure conditions, an increase in the temperature from 200 to 300 ºC leads to improvements in the bio-oil and aqueous fraction yields at the expenses of the solid yield. This accounts for the positive kinetic effect of the temperature depolymerisation, deamination, decomposition and re-polymerisation reactions (Dimitriadis and Bezergianni, 2017; Gollakota et al., 2018; Kumar et al., 2018; Thiruvenkadam et al., 2015).

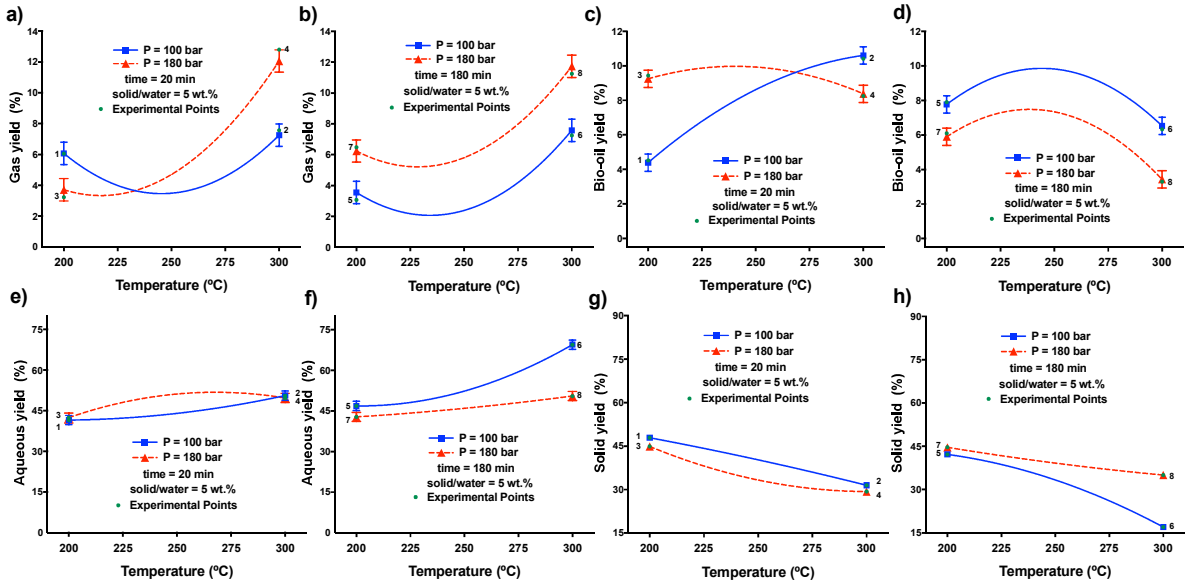

Figure 2. Interaction plots showing the effects of the processing conditions on the global reaction products using a solid/water ratio of 5 wt.%. Error bars display 95% confidence intervals.

Augmenting the pressure alters the impact of the temperature on the process. While at low temperature (200-250 ºC), augmenting the pressure from 100 to 180 bar upsurges the bio-oil yield, depleting the gas yield, at high temperature (250-300 ºC), this same increase in the pressure translates into a considerable increase in the yield to gas along with a decrease in the formation of bio-oil. Irrespective of the temperature of the process, this pressure increase translates into an increase in the aqueous fraction yield at the expenses of the solid yield. These differences might be the outcome of the beneficial kinetic impact of the pressure on the process, which favours liquefaction, thus increasing the bio-oil yield at low temperature, conditions at which gas formation is not promoted. Besides, this pressure increase also can promote the bio-oil transformation into gaseous species (Gollakota et al., 2018) at high temperature due to the synergistic effect of temperature and pressure and the positive influence of the temperature on the transformation of bio-oil into gaseous species. Precisely, intensifying the total pressure upsurges the partial pressure of biomass decomposition products, i.e., intermediate reactive fragments/species inside the reactor. This also facilitates the penetration of water into the almond hulls core structure, thus promoting hydrolysis reactions to take place to a greater extent (Dimitriadis and Bezergianni, 2017; Gollakota et al., 2018; Kumar et al., 2018; Thiruvenkadam et al., 2015). Besides, this increase in the pressure also upsurges the auto-dissociation of water (Schienbein and Marx, 2020), as the conditions are closer to the supercritical point of water, which also facilitates hydrolysis reactions. Such increase also aids to polarise water, thus augmenting the protons concentration in the reaction medium, which endorses

reactions catalysed by acid species. These developments change the effect of the temperature at high pressure. In particular, at 180 bar, increasing the temperature substantially increases the gas yield (especially between 250 and 300 ºC) and decreases the solid yield, with the bio-oil and aqueous fraction yield being practically unaffected. Therefore, these phenomena are accounted for by the positive kinetic influence of the reaction temperature and pressure, which favours water penetration into the biomass, on hydrolysis and decarboxylation reactions (Dimitriadis and Bezergianni, 2017; Gollakota et al., 2018; Kumar et al., 2018; Thiruvenkadam et al., 2015).

The outcome of the reaction time for a diluted suspension (5 wt.%) can be gathered by comparing Figure 2 a/c/e/g and b/d/f/h. The influence of the reaction time depends on the temperature and pressure. At low pressure (100 bar), the reaction time exerts a significant influence on the bio-oil, aqueous fraction and solid yields, while the gas yield is unaffected. At low temperature (200-250 ºC), prolonging the reaction time leads to an increase in the bio-oil yield together with a soft decrease in the liquid yield, without substantially modifying the solid yield. These variations are thought to be a result of the beneficial kinetic impact of the reaction time, which increases biomass transformation into bio-oil (Dimitriadis and Bezergianni, 2017; Gollakota et al., 2018; Kumar et al., 2018; Thiruvenkadam et al., 2015), without promoting its further decomposition to gas and/or solid products. At 180 bar, the influence of the reaction time depends on the temperature. Accurately, the gas yield substantially increases with prolonging the reaction time from 20 to 180 min, especially at temperatures between 200 and 250 ºC. Besides, this increase in the reaction time leads to depletions in the yields to bio-oil and liquid along with an upturn in the solid yield, regardless of the temperature.

Therefore, the experimental results indicate that the aqueous liquid product and bio-oil evolve into hydro-char when using long reaction times due to a more significant spread of carbonisation reactions, which are favoured at long reaction times (Saqib et al., 2019). These developments alter the outcome of the temperature and pressure when prolonged (180 min) reaction durations are applied. In particular, irrespective of the pressure, while augmenting the reaction temperature from 200 to 250 ºC does not markedly affect the distribution of the products, a further increase from 250 to 300 ºC increases the aqueous liquid and gas yield at the expenses of the bio-oil and solid yields since gas formation is

preferential at elevated temperature and using lengthy reaction times (Gollakota et al., 2018). Besides, part of the bio-oil could be converted to gas under such conditions. An increase in the pressure from 100 to 180 bar leads to a proliferation in the gas yield and decreases in the bio-oil and aqueous product yields due to the beneficial kinetic impact of the pressure on decarboxylation, depolymerisation and deamination reactions leading to the gas formation (Gollakota et al., 2018). These results are in concordance with the thermodynamics of this thermochemical route, which displays an endothermic nature at low temperatures and exothermic character at high temperatures (Kumar et al., 2018; Muppaneni et al., 2017). As a result, the production of gas, liquid and bio-oil increases when the process temperature increases and reaches a point after which an additional extent inhibits liquefaction.

Increasing the solid loading changes the impact of the temperature, pressure and reaction time. When a solid loading of 25 wt.% is used (Figure 3), the impact of the temperature strongly relies on the reaction time. For a 20 min treatment, the effect of the temperature on the gas and bio-oil yields does not rely on the pressure, and the same evolutions are observed within the whole range of pressure (100-180 bar). An increase in the temperature between 200 and 250 ºC leads to an increase in the gas production along with a decrease in the bio-oil yield, which suggests that part of the bio-oil is being converted into gas by cracking and/or pyrolysis, as these reactions prevail over hydrolysis when using high solid/water ratios (Dimitriadis and Bezergianni, 2017; Gollakota et al., 2018; Xu and Lancaster, 2008). A subsequent increase from 250 to 300 ºC increases the bio-oil yield without markedly modifying the gas yield, conditions at which increasing the pressure from 100 to 180 bar leads to small increases and decreases in the gas and bio-oil yield, respectively. Conversely, the aqueous liquid fraction and solid yields are strongly affected by the pressure. Whilst, at low pressure (100 bar), an increase in the temperature does not remarkably change the yields to these fractions; a small increase is observed for the aqueous product happening along with a minor decrease in the solid yield. An increase in the pressure from 100 to 180 bar significantly increases the solid yield at the expenses of the liquid yield, with these variations being notably marked between 200 and 250 ºC. As a result, at 180 bar, increasing the temperature leads to a substantial decrease in the solid yield accompanied by a prominent increase in the aqueous product yield. The combination of high temperature and pressure using concentrated suspensions favours the hydro-

char production by repolymerisation, crystallisation and/or condensation reactions (Dimitriadis and Bezergianni, 2017; Gollakota et al., 2018; Xu and Lancaster, 2008).

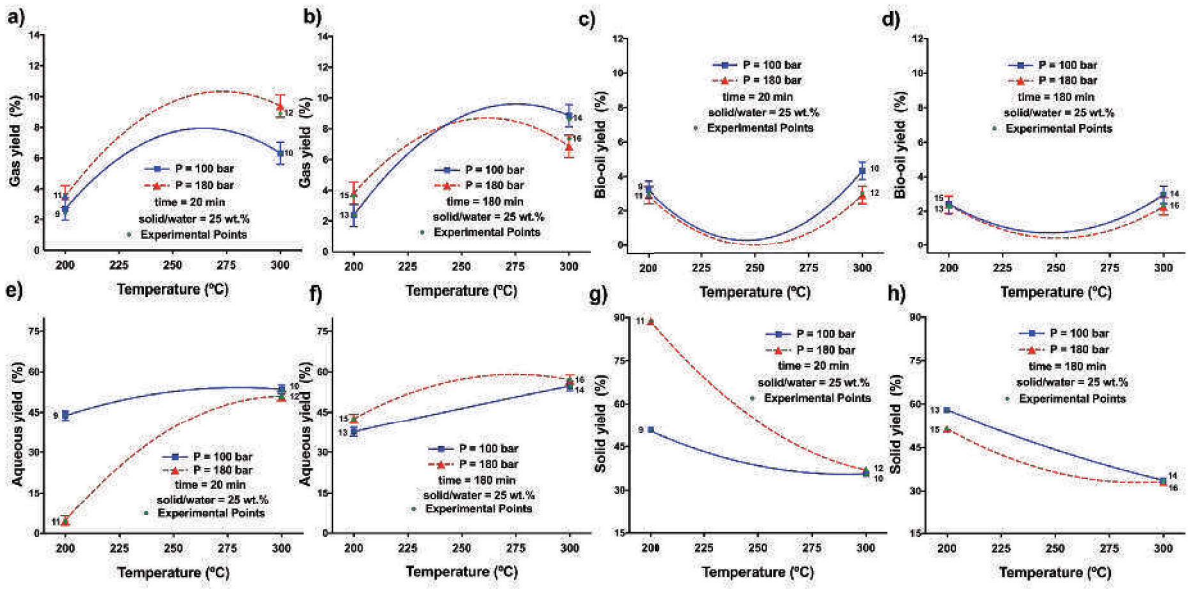

Figure 3. Interaction plots showing the effects of the processing conditions on the global reaction products using a solid/water ratio of 25 wt.%. Error bars display 95% confidence intervals.

The effect of the reaction time for a solid/water ratio of 25 wt.% primary depends on the pressure. For low pressure (100 bar), an increase from 20 to 180 min leads to a rise in the gas yield at the expenses of the bio-oil yield, especially at high temperature (230-300 ºC). An increase in the reaction time promotes the transformation of bio-oil into gases (Dimitriadis and Bezergianni, 2017; Gollakota et al., 2018; Kumar et al., 2018; Thiruvenkadam et al., 2015). The aqueous product and solid yield are less affected by the reaction time at low pressure, and only small variations are observed at low temperature (200-250 ºC). In particular, increasing the reaction time from 20 to 180 min leads to a decrease in the aqueous product yield and a rise in the solid yield, as hydrothermal carbonisation reactions are favoured at low temperature and long reaction times (Dimitriadis and Bezergianni, 2017; Gollakota et al., 2018; Xu and Lancaster, 2008). At high pressure (180 bar), the evolutions observed for the aqueous product yield with enlarging the reaction time are more manifest. As a result, when the treatment is conducted for 180 min, the effect of the pressure is less significant as the beneficial kinetic impact of the former can compensate for the impact of the latter. Unrelatedly of the pressure, increasing the temperature leads to an increase in the gas yield (especially between 200 and 250 ºC) at the expenses of the solid yield. These variations might be accounted for by the high solid/water ratio used, as high solid loadings favour a greater spread of

thermal decomposition and pyrolysis reactions at the expenses of hydrolysis reactions, thus promoting gas formation at these reaction conditions (Dimitriadis and Bezergianni, 2017; Gollakota et al., 2018; Xu and Lancaster, 2008). Besides, the bio-oil yield is meagre (2-3 wt.%) irrespective of the other operating conditions, as the use of long reaction times promotes bio-oil transformation into gaseous species.

3.2.2 Chemical composition and LHV of the gas phase

The gas-phase produced during the HTT of almond hulls comprises a mixture of H_2 (1-16 vol.%), CO_2 (37-97 vol.%), CO (0-31 vol.%) and CH_4 (0-29 vol.%), with a LHV shifting between 1 and 13 MJ/m^3 STP. The ANOVA analysis reveals that the operating conditions exert a statistically significant influence on the composition of the gas and its LHV. The complete influence of the conditions determined by the cause-effect Pareto test (Table S2) is included as supplementary information. Figures 4 and 5 show the effects of the temperature at 100 and 180 bar for a reaction time of 20 and 180 min on the composition and LHV of the gas phase, using a solid loading of 5 wt.% and 25 wt.%, respectively.

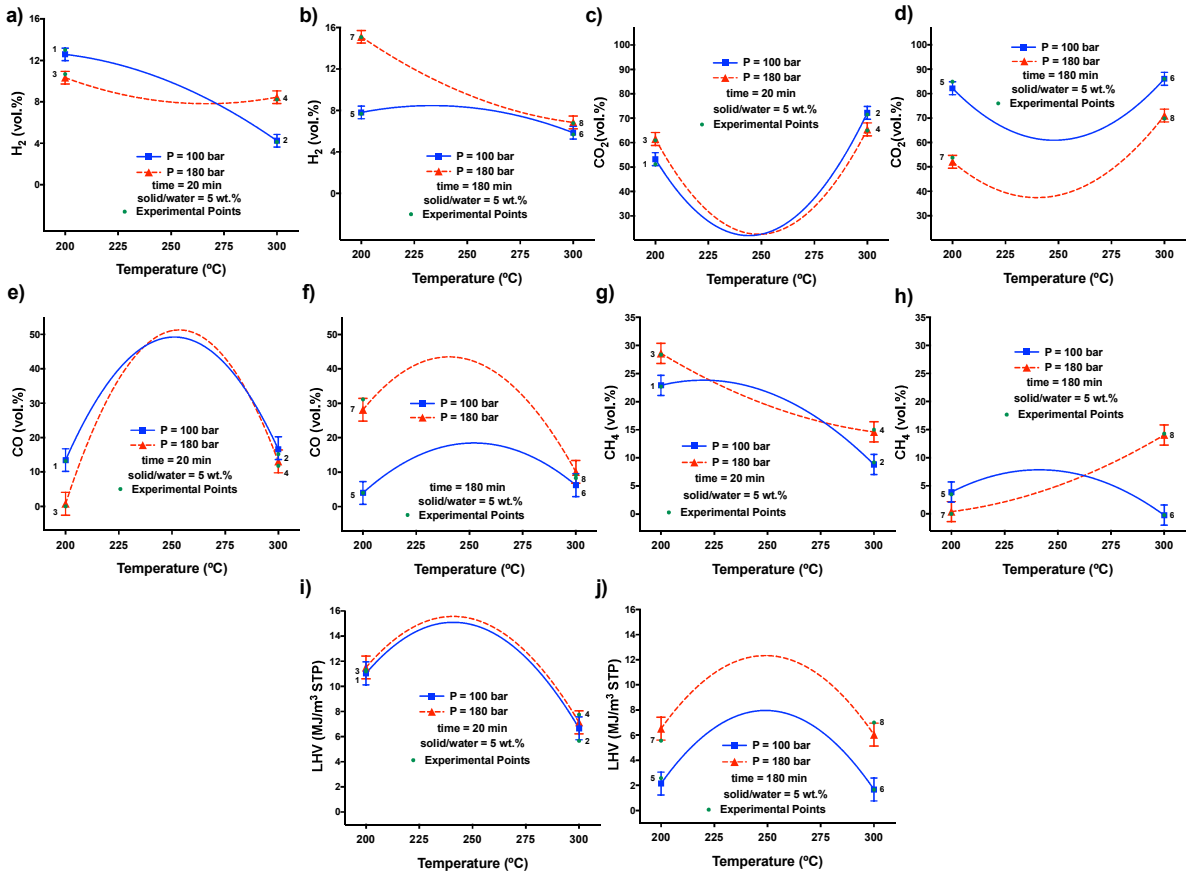

Figure 4. Interaction plots showing the effects of the processing conditions on the composition and LHV of the gas using a solid/water ratio of 5 wt.%. Error bars display 95% confidence intervals.

387 The outcomes of the temperature, pressure and reaction time on the gas composition and LHV depend on
388 the solid/water ratio. Figure 4 shows that when employing diluted suspension (5 wt.%), the reaction time
389 alters the impact of the temperature. For a rapid treatment (20 min), the impact of the pressure is feeble,
390 and the gas composition and LHV mostly rely on the temperature; CO_2 and CO being the species more
391 affected by such variations. In particular, a preliminary upsurge in the temperature between 200 and 250
392 ºC leads to a decrease in the relative amount of CO_2 along with an increase in the proportion of CO. A
393 further rise in the temperature results in the opposite trend; i.e., the relative amount of CO_2 increases while
394 the proportion of CO falls down. The relative amounts of H_2 and CH_4 decrease with increasing the
395 temperature from 200 to 300 ºC. These variations result in a preliminary improvement of the gas LHV
396 between 200 and 250 ºC, continued by a decline with a continuous augment in the reaction temperature
397 up to 300 ºC. At low temperature, the water gas shift ($CO+H_2O \Leftrightarrow CO_2+H_2$) and methane reforming
398 ($CH_4+H_2O \Leftrightarrow CO+3H_2$) reactions are shifted towards the formation of CO_2. Increasing the temperature
399 between 200 and 250 ºC leads to an increase in the proportion of CO and decreases in the relative amounts
400 of CO_2, CH_4 and H_2 due to the exothermicity of the former and endothermicity of the latter reaction
401 (Remón et al., 2016a; Remón et al., 2016b; Remón et al., 2015). However, an increase between 250 and
402 300 ºC promotes a greater spread of decarboxylation, via pyrolysis, thermal decomposition and cracking
403 reactions, which results in a gas product primarily made up of CO_2 (Dimitriadis and Bezergianni, 2017;
404 Gollakota et al., 2018; Xu and Lancaster, 2008).
405
406 The pressure alters the effect of the reaction time. On the one side, at low pressure (100 bar), increasing
407 the reaction time from 20 to 180 min (Figure 4 a/c/e/g vs b/d/f/h) reduces the proportions of H_2, CO and
408 CH_4 and upsurges the concentration of CO_2 in the gas. This leads to a decrease in its LHV as
409 decarboxylation reactions are promoted with increasing the reaction time, thus resulting in a gas mainly
410 consisting of CO_2. These variations are more critical between 200 and 280 ºC and might be the outcome
411 of the governing secondary decomposition and Bourdard ($2CO_2 \Leftrightarrow CO+C$) gas reactions, which promote
412 CO_2 formation (Dimitriadis and Bezergianni, 2017; Gollakota et al., 2018; Xu and Lancaster, 2008). On
413 the other, at high pressure (180 bar), this same process duration increment vaguely upturns the proportion
414 of H_2 and drops the relative amount of CH_4, without substantially modifying the relative amounts of CO_2
415 or CO in the gas product. As a result of these variations, for a long reaction time, the gas composition is

affected by the total pressure, and different changes with the temperature happen for some gases. In particular, the effect of the temperature for the relative amounts of H_2 and CH_4 depends on the total pressure. At low pressure (100 bar), the relative amounts of H_2 and CH_4 are not substantially affected by the temperature. In comparison, at high pressure (180 bar), increasing the temperature drops the relative amount of H_2 at the expenses of the proportion of CH_4 in the gas. As the pressure increases, the methane reforming reaction shifts towards the left (CH_4 formation) due to the lower amount of gaseous species according to the Equilibrium Law (Le Chatelier's Principle).

Conversely, the effect of the temperature is not affected by the total pressure for the proportions of CO_2 and CO in the gas. Irrespective of the pressure, an initial increase in the temperature between 200 and 250 ºC leads to a decrease in the proportion of CO_2 along with an increase in the relative amount of CO. A further increase up to 300 ºC rises and drops the proportions of CO_2 and CO in the gas, respectively. This could be explained by the thermodynamics of the water-gas shift and methane reforming reactions and the kinetic effect of the temperature, which promotes decarboxylation reactions at high temperatures as described earlier. As a result, the LHV of the gas displays a first increase with the temperature between 200 and 250 ºC, followed by a subsequent depletion as the temperature increases up to 300 ºC. Besides, increasing the total pressure has a significant impact on the gas phase composition; CO_2 and CO being the species most affected by such variation. For these two gases, increasing the pressure from 100 to 180 bar leads to a decrease in the relative amount of CO_2 together with an increase in the proportion of CO as the Bourdard reaction shifts towards CO formation as the pressure increases. Besides, this pressure increment slightly increases both the proportion of H_2 at low temperature (200-230 ºC) and the proportion of CH_4 at high temperature (275-300 ºC). These variations also result in an enhancement of the LHV of the gas with increasing the pressure from 100 to 180 bar regardless of the temperature.

Increasing the solid/water ratio from 5 to 25 wt.% modifies the composition and LHV of the gas phase, which is primarily made up of CO_2 (>70 vol.%) irrespective of the conditions (Figure 5). In general, an increase in the solid loading leads to a decrease in the relative amount of H_2 in the gas, along with an increase in the proportion of CO_2 (Figure 4 vs Figure 5). This is accounted for by a more significant extension of decarboxylation, thermal cracking and pyrolysis reactions over hydrolysis and

depolymerisation reactions, thus leading to CO_2 formation when high solid loadings are used (Egües et al., 2010; Pińkowska et al., 2014). The effects of the temperature and pressure for a concentrated suspension depend on the reaction time (Figure 5). For a short reaction time, the impact of the pressure is relatively weak, and the gas composition is mostly affected by the temperature. Precisely, irrespective of the pressure, augmenting the temperature between 200 and 250 ºC leads to drops in the proportion of H_2 and CH_4 along with an upturn in the relative amount of CO, without substantially influencing the composition of CO_2, due to the thermodynamic nature of the water-gas shift and methane reforming reactions (Remón et al., 2016a; Remón et al., 2016b; Remón et al., 2015). A subsequent increase up to 300 ºC marginally increases the proportion of H_2 and declines the relative amount of CO, without extensively modifying the relative amounts of CO_2 or CH_4. The LHV of the gas is very low due to the considerable proportion of CO_2 in the mixture. Increasing the temperature produces a depletion in the LHV of the gas due to the increase observed in the relative amount of CO_2. The effect of the pressure is feeble, and it is more critical at low than at high temperature. In particular, between 200 and 250 ºC, an increase from 100 to 180 leads to decreases in the proportions of H_2 and CO_2 along with increases in the relative amount of CO and CH_4.

The effect of the reaction time depends on the pressure. At low pressure (100 bar), the impact of the reaction time is weak, and it is only significant at low temperature (200-250 ºC). At such temperatures, prolonging the reaction time from 20 to 180 min increases the proportions of H_2 and CO at the expenses of the relative amounts of CO_2 and CH_4, which, leads to a small decrease in the LHV of the gas. Conversely, when a high pressure (180 bar) is used, this same temperature intensification mainly increases the relative amount of CO_2 in the gas at the expenses of the other gases. As a result, the gas phase primarily consists of CO_2, and the LHV of the gas is very low, as thermal cracking, pyrolysis and decarboxylation reactions are promoted using long reaction times (Dimitriadis and Bezergianni, 2017; Gollakota et al., 2018; Xu and Lancaster, 2008). Irrespective of the pressure, H_2 and CO_2 are the species most affected by the reaction temperature for a concentrated suspension using a long reaction time. In particular, an increase in the temperature increases the relative amount of CO_2 and decreases the proportion of H_2, which leads to a decrease in the gas LHV as explained above. Also, rising the pressure leads to the same variations; i.e., the proportion of CO_2 augments and the relative amount of H_2 decreases,

474 which drops the LHV of the gas due to the beneficial impacts of the temperature and reaction time on
475 decarboxylation.
476

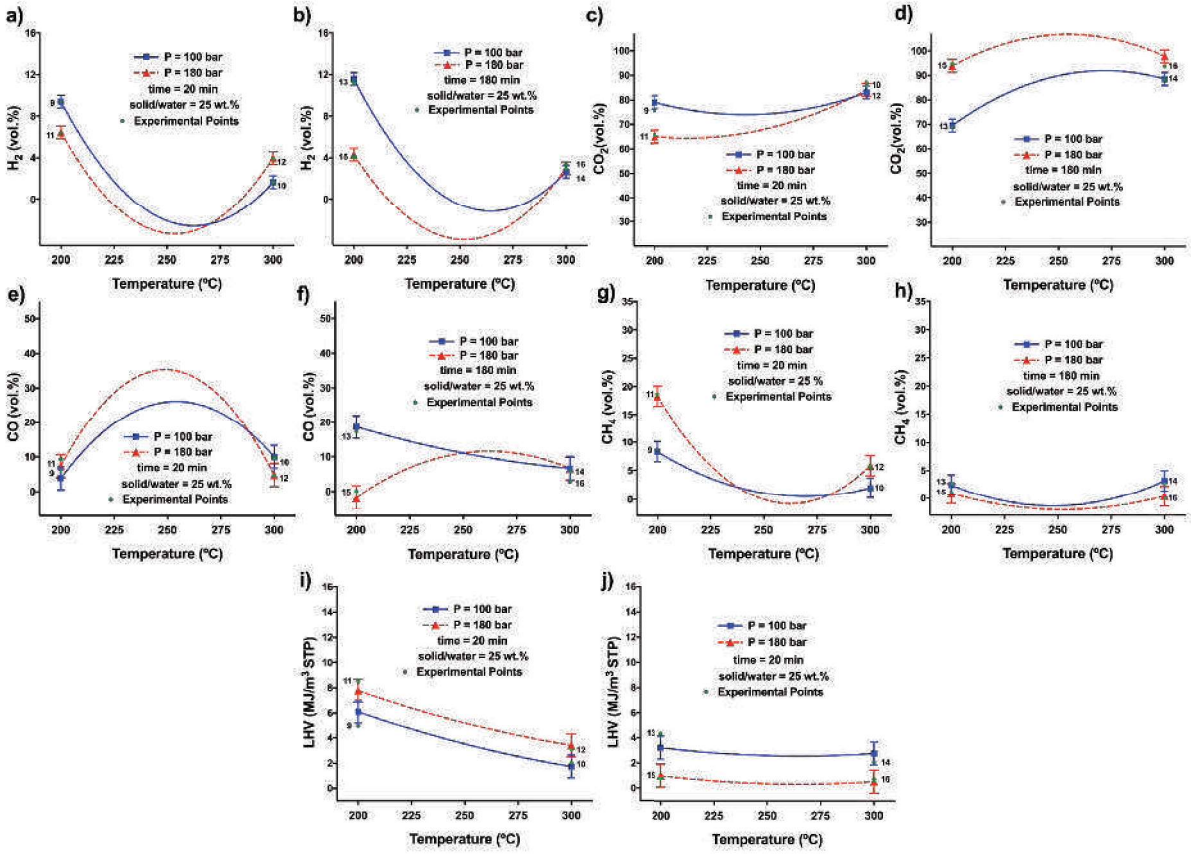

477

478 *Figure 5. Interaction plots showing the effects of the processing conditions on the composition and LHV*
479 *of the gas using a solid/water ratio of 25 wt.%. Error bars display 95% confidence intervals.*
480

481 **3.2.3 Elemental composition and HHV of the bio-oil**

482 The concentrations of C, H, O and N in the bio-oil vary between 57-74 wt.%, 5-6 wt.%, 18-38 wt.% and
483 1-3 wt.%, respectively, while its HHV moves between 21 and 31 MJ/kg. The ANOVA of the results
484 reveals that the operating conditions and several interactions between operating variables exert a
485 significant influence on these properties. The complete influence of the conditions determined by the
486 cause-effect Pareto test (Table S2) is included as supplementary information. Figure 6 shows the effects
487 of the temperature at 100 and 180 bar for a reaction time of 20 and 180 min on the elemental composition
488 and HHV of the bio-oil, using a solid loading of 5 wt.%. These effects are plot in Figure 7 for a solid
489 loading of 25 wt.%.
490
491

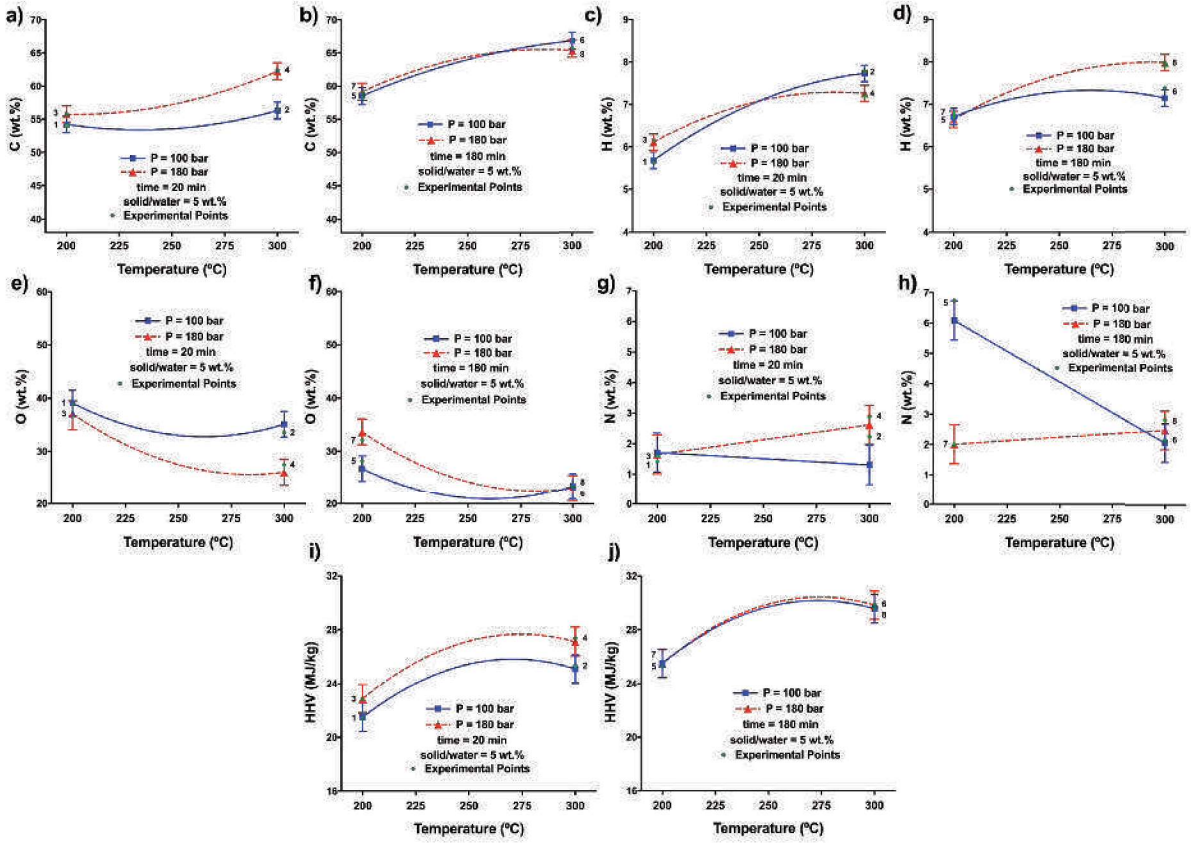

492

493 *Figure 6. Interaction plots showing the effects of the processing conditions on the composition and HHV*
494 *of the bio-oil using a solid/water ratio of 5 wt.%. Error bars display 95% confidence intervals.*
495

496 The reaction duration substantially influences the relative influence of the reaction temperature on the
497 elemental composition and HHV of the bio-oil. For a short reaction time (20 min) analogous trends are
498 observed for the reaction temperature regardless of the total pressure or solid/water ratio. In particular,
499 an initial increase in the temperature leads to a small increase in the proportion of C in the bio-oil together
500 with quite a pronounced increase in the proportion of H and a substantial decrease in the relative amount
501 of O; with these variations increasing the HHV of the bio-oil. A further temperature raise up to 300 ºC
502 does not substantially modify the bio-oil elemental composition or its HHV; this latter property displaying
503 a plateau between 250 and 300 ºC. As an exception, only a small increase in the proportion of C is
504 observed. Besides, under these reaction conditions, the bio-oil contains a small percentage of N
505 compounds, which slightly increases with augmenting the temperature or the solid/water ratio. The
506 increases observed in the relative amounts of C and H, together with the decreases observed for the
507 proportion of O in the bio-oil are accounted for by the beneficial impact of the temperature on the process.
508 This beneficial temperature influence makes it possible that deoxygenation, deamination and thermal
509 cracking reactions occur to a greater extent (Duan et al., 2013; Duan and Savage, 2011a; Duan and
510 Savage, 2011b; Fisk et al., 2009), as they are enhanced at high temperature. The effect of the pressure is

feeble and depends on the temperature and solid/water ratio. For a low solid/water ratio (5 wt.%) the pressure only exerts a significant influence at high temperature (250-300 ºC). An increase from 100 to 180 bar leads to a rise in the proportion of C along with a decline in the concentration of O, which enhances the bio-oil HHV.

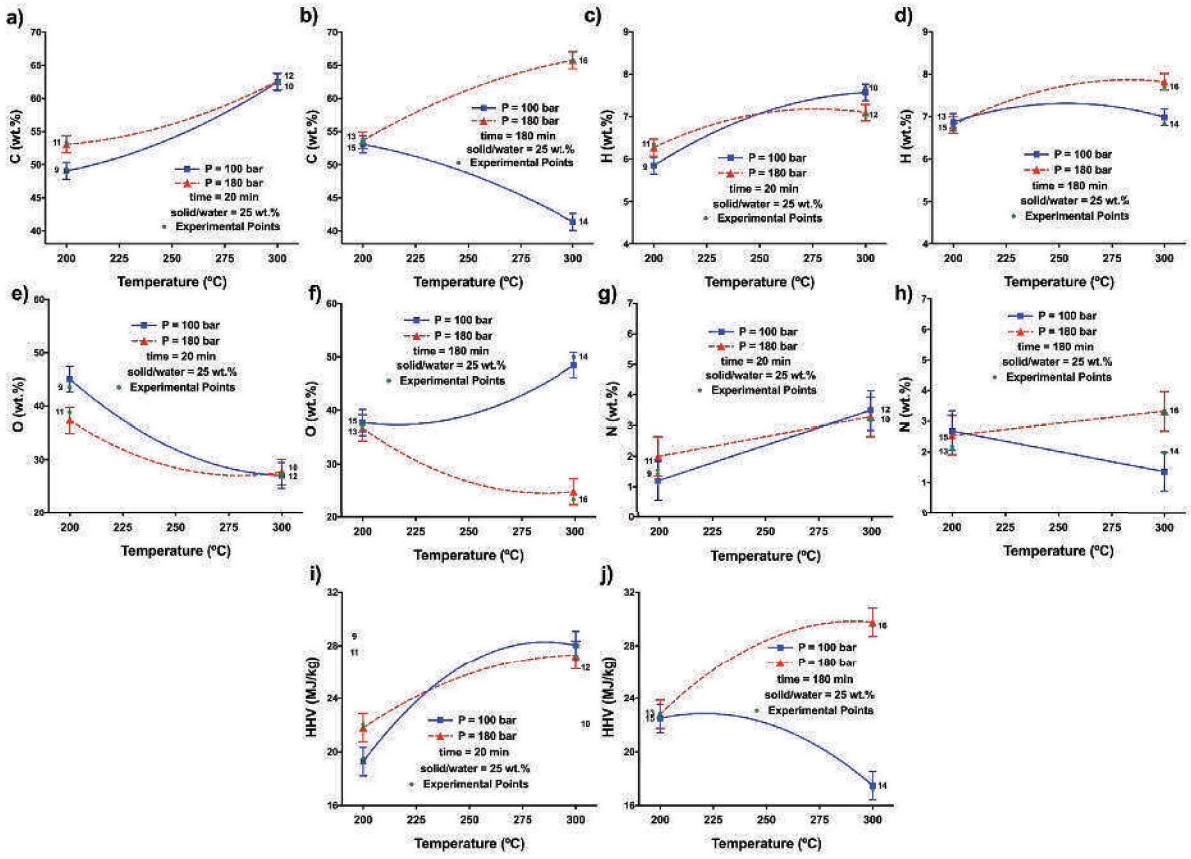

Figure 7. Interaction plots showing the effects of the processing conditions on the composition and HHV of the bio-oil using a solid/water ratio of 25 wt.%. Error bars display 95% confidence intervals.

Conversely, Figure 7 shows that for a concentrated suspension (25 wt.%) these developments take place at low temperature (200-250 ºC). The pressure exerts a positive kinetic influence on the process, increasing the partial pressure of the reactive species inside the reactor. Besides, it also promotes water penetration into biomass, thus increasing its reactivity. For a speedy treatment, the influence of the solid loading is not very important and minimal variations for the bio-oil elemental composition and HHV take place. These variations are only significant for the proportions of C and O. Between 200 and 250 ºC, increasing the solid/water ratio from 5 to 25 wt.% (Figure 6 vs Figure 7) decreases the relative amount of C at the expenses of the proportion of O, which results in a decrease in the HHV of the bio-oil. Conversely, between 250 and 300 ºC, the effect of the solid/water ratio depends on the pressure. At low pressure (100

529 bar) increasing the solid loading upsurges the proportion of C and drops the relative amount of O, which
530 enhances the bio-oil HHV. However, as the pressure increases, the effect of the solid/water ratio becomes
531 less and less important. As a result, at high pressure (180 bar) it does not meaningfully affect the elemental
532 composition of the bio-oil or its HHV.
533
534 Different evolutions for the elemental composition of the bio-oil are observed depending on the
535 solid/water ratio. For a solid/water ratio of 5 wt.% (Figure 6), prolonging the reaction time from 20 to
536 180 min rises the relative amount of C and drops the proportion of O in the bio-oil, with these variations
537 resulting in an increase in the HHV of this product irrespective of the total pressure. The proportions of
538 H and N in the bio-oil are less affected. In particular, this same increase in the reaction time increases the
539 percentage of H very slightly at low temperature and pressure. Also, it leads to an increase in the
540 proportion of N in the bio-oil at low pressure. As a result, the effects of the temperature and pressure
541 using a diluted suspension for a long reaction time (5 wt.% and 180 min) are very similar to those
542 described for a 20 min reaction time; i.e., increasing the temperature leads to increases in the proportion
543 of C and H along with a decrease in the proportion of O, thus leading to a rise in the bio-oil HHV. Besides,
544 the effect of the pressure is not very important as a practical matter. Small variations occur for the relative
545 amount of O and N at low temperature and the relative amount of H in the bio-oil at high temperature.
546 Increasing the reaction time favours bio-oil transformation into a gas via decarboxylation and thermal
547 cracking as described earlier, thus augmenting the C content and enhancing the HHV, decreasing the
548 concentration of O in the bio-oil (Dimitriadis and Bezergianni, 2017; Gollakota et al., 2018; Xu and
549 Lancaster, 2008).
550
551 Contrariwise, when a solid/liquid ratio of 25 wt.% is used (Figure 7), the effect of the reaction time
552 depends on the pressure. At low pressure (100 bar), increasing the reaction time decreases the proportions
553 of C and N and increases the relative amount of O, with the percentage of H being unaffected. Increasing
554 the reaction time promotes bio-oil transformation into gaseous products via reforming, pyrolysis and/or
555 thermal cracking. Therefore, bio-oil light oxygenates can be removed, which might result in a bio-oil
556 with a high oxygen content. At high pressure, the chemical composition of bio-oil and its HHV are mostly
557 unaffected by the reaction time. As a result, for a long reaction time, the effects of the temperature depend

558 on the pressure with two different evolutions taking place. On the one hand, at low pressure (100 bar),
559 the relative amount of C diminishes and the proportion of O upsurges, leading to a reduction in the bio-
560 oil HHV, with augmenting the reaction temperature from 200 to 300 ºC. On the other, at high pressure
561 (180 bar), this same temperature increment upsurges and reduces the proportions of C and O, respectively,
562 which leads to an increase in the bio-oil HHV. Besides, the effect of the pressure is only essential when
563 a concentrated suspension is employed for a prolonged reaction time. An increase from 100 to 180 bar
564 leads to a rise in the proportion of C along with a decrease in the relative amount of O, thus substantially
565 increasing the HHV of the bio-oil resulting from the beneficial kinetic impact of the pressure on
566 deoxygenation, decarboxylation and dehydration reactions under such conditions, as they lead to
567 increases in the amount of C and decreases in the proportion of O in the bio-oil (Duan et al., 2013; Duan
568 and Savage, 2011a; Duan and Savage, 2011b; Fisk et al., 2009). Besides, these variations depend on the
569 temperature, and the higher the temperature, the sharper these variations are (Duan et al., 2013; Duan and
570 Savage, 2011a; Duan and Savage, 2011b; Fisk et al., 2009).
571
572 **3.2.4 Chemical composition of the bio-oil**
573 The bio-oil is made up of a complex mixture of several oxygenated compounds, which relative amount
574 (expresses as relative chromatographic area) vary as follows. Alkanes (0-14%), aldehydes (0-7%),
575 carboxylic acids (0-3%), ketones (0-49%), phenols (0-49%), alcohols (0-3%), furans (0-29%), benzenes
576 (0-40%) and cyclic (0-3%) and nitrogen (4-82%) compounds. The detailed chemical composition is
577 provided as supplementary material in Table S3. The ANOVA analysis reveals that the operating
578 conditions, along with several interactions between them, exert a significant influence on the chemical
579 composition of the bio-oil. The complete influence of the conditions determined by the cause-effect
580 Pareto test (Table S2) is included as supplementary information. Figure 8 shows the effects of the
581 temperature at 100 and 180 bar for a reaction time of 20 and 180 min on the relative amounts of alkanes,
582 ketones, phenols, furans, nitrogen compounds and benzenes in the bio-oil, using a solid loading of 5 wt.%.
583 These effects are plot in Figure 9 for a solid loading of 25 wt.%.
584
585 The solid/water ratio modifies the effect of the temperature. When a solid loading of 5 wt.% is used
586 (Figure 8), the impact of the processing temperature is not influenced by the reaction time or pressure,

and similar evolutions with the temperature are observed. In particular, an initial increase from 200 to 250 ºC leads to improvements in the proportions of ketones and phenols along with decreases, primarily, in the relative amount of nitrogen compounds, and to a lesser extent, in the proportion benzenes. Besides, the proportion of alkanes slightly increases only when a short reaction time is used (20 min), while the relative amount of furans decreases when a quick reaction time (20 min) is used at high pressure (180 bar). However, these latter variations are not essential from a practical standpoint. A subsequent increase in the temperature also leads to a decrease in the proportion of nitrogen compounds, while the proportion of benzenes increases at the expenses of the relative amounts of ketones and alkanes (at short reaction times) or phenols (at long reaction times). These results suggest that the bio-oil obtained at low temperature comprises compounds of high molecular mass that cannot be detected and/or quantified by gas chromatography. This bio-oil is also rich in nitrogen derived compounds extracted from the protein content of the biomass via solvolysis and contains a small proportion of benzenes resulted from lignin depolymerisation (Lorente et al., 2019; Remón et al., 2019c).

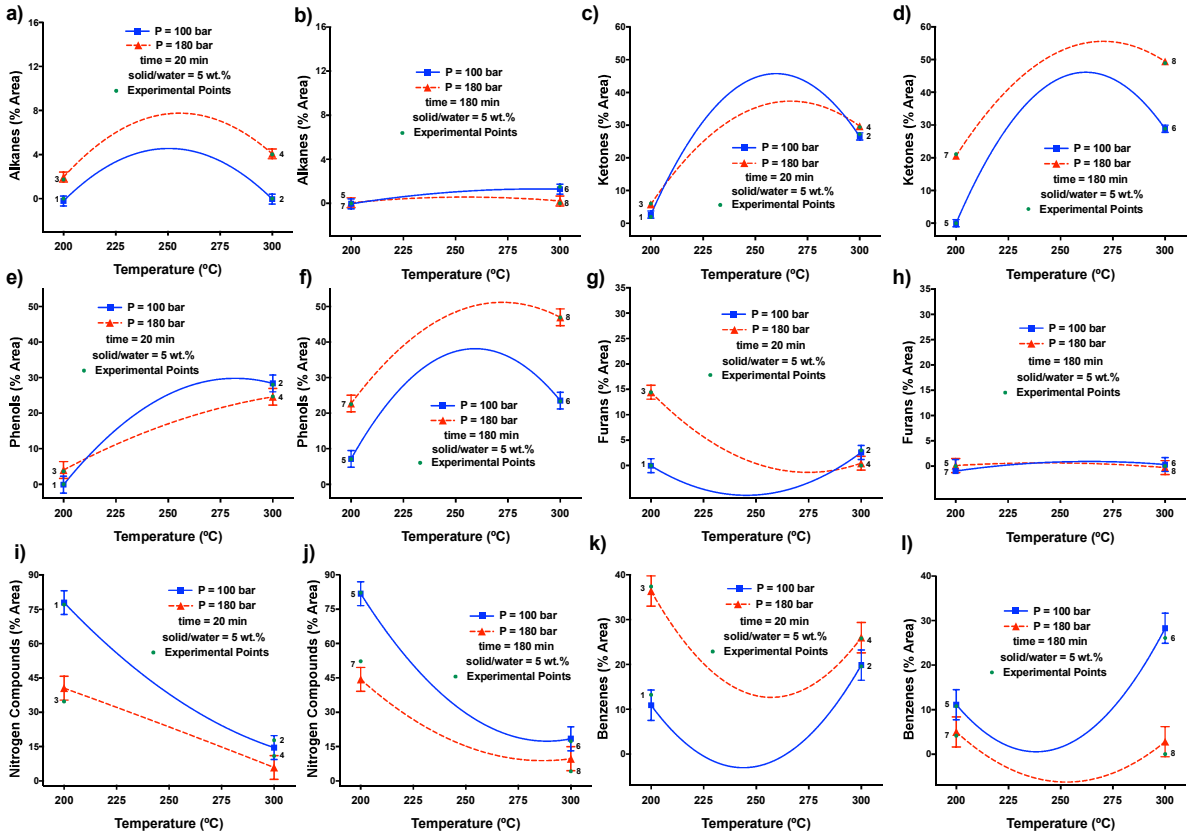

Figure 8. Interaction plots showing the effects of the processing conditions on the chemical composition of the bio-oil using a solid/water ratio of 5 wt.%. Error bars display 95% confidence intervals.

605

606 However, as the temperature increases, hydrolysis, depolymerisation and recombination reactions are
607 promoted (Duan et al., 2013; Duan and Savage, 2011a; Duan and Savage, 2011b; Fisk et al., 2009). This
608 aids to the hydrolysis of biomass bio-polymers into high molecular weight, water-soluble oligomers and
609 their subsequent rupture into reactive species, primarily comprising small oxygenated compounds
610 (Kumar et al., 2018; Yang et al., 2018), thus increasing the relative amount of alkanes, ketones and
611 phenols in the bio-oil. As such, the relative amount of benzenes in the liquid decreases due to the increase
612 in the proportion of small oxygenates in the bio-oil. Besides, increasing the temperature also promotes
613 proteins decomposition to gaseous products by deamination and decarboxylation (Egües et al., 2010;
614 Pińkowska et al., 2014), thus decreasing the relative amount of nitrogen derived compounds. A further
615 increase in the temperature promotes the transformation of some bio-oil oxygenates into gaseous
616 products, thus proving evidence for the decreases occurring in the relative amounts of ketones and
617 phenols, which leads to an increase in the proportion of benzenes.
618

619 The effects of the reaction time depend on the pressure. On the one hand, at 100 bar, the reaction time
620 does not exert a great influence on the bio-oil chemical composition. Conversely, at high pressure (180
621 bar), regardless of the temperature, increasing the reaction time increases the proportions of ketones and
622 phenols and decreases the relative amounts of alkanes, furans and benzenes; the proportion of nitrogen
623 compounds being practically unaltered. During biomass HTT, biomass polysaccharide structural
624 components (cellulose and hemicellulose) decompose towards the formation of ketones and phenolic
625 compounds via isomerisation, cyclisation and dehydration reactions (Kumar et al., 2018; Yang et al.,
626 2015). Therefore, these reactions might be promoted by the positive effect of the pressure and the reaction
627 time, thus augmenting the proportions of these species in the bio-oil. As a result of this, the effect of the
628 pressure becomes more important as the reaction time increases. In particular, for a quick treatment (20
629 min), an increase in the pressure from 100 to 180 bar leads to an increase in the relative amount of
630 benzenes along with small increases in the proportions of alkanes and furans, at the expenses of the
631 relative amount of nitrogen compounds in the bio-oil. For a long reaction time (180 min), this same
632 increase in the pressure substantially increases the relative amounts of ketones and phenols and decreases
633 the proportions of nitrogen compounds and benzenes. The pressure exerts a positive effect on lignin

depolymerisation reactions, which might result in an increase in the proportion of benzenes in the bio-oil when a short reaction time is used. Besides, the positive effect of the reaction time leads to a more significant development of isomerisation, cyclisation and dehydration reactions (Kumar et al., 2018; Yang et al., 2015), which leads to an increase in the proportion of ketones and phenols using long reaction times.

For a concentrated suspension (25 wt.% solid loading, Figure 9), the reaction time alters the effect of the temperature. For a short reaction time (20 min), irrespective of the pressure, an increase in the temperature between 200 and 270 ºC leads to improvements in the proportions of ketones and phenols together with decreases in the relative amounts of furans and benzenes. This is accounted for by the positive effect of the temperature on isomerisation, cyclisation and dehydration reactions (Kumar et al., 2018; Yang et al., 2015) of the reactive fragments produced from the carbohydrate matter of almond hulls. A subsequent increase up to 300 ºC decreases the relative amounts of ketones, furans and nitrogen compounds. This substantially increases the proportion of benzenes in the bio-oil due to the gradual transformation of part of the bio-oil into gaseous products at high temperature (Lorente et al., 2019; Remón et al., 2019c). An exception to this occurs for the relative amount of alkanes, which displays a decrease with the temperature only at low pressure. For a lengthy treatment, the temperature exerts a significant influence on the proportions of ketones, phenols and benzenes. Irrespective of the pressure, an increase between 200 and 280 ºC leads to increases in the relative amounts of ketones and phenols and the expenses of the proportion of benzenes, due to the positive effect of the temperature on the process, as described earlier. A subsequent increase up to 300 ºC increases the relative amount of the latter and decreases the proportion of the former, as the use of high temperatures for a long reaction time promotes bio-oil transformation into gaseous products as described above. The effect of the pressure for a concentrated suspension depends on the reaction time, with more critical variations taking place for a short than for a long reaction time. In particular, for a reaction time of 20 min, an increase from 100 to 180 bar increases the proportions of furans and nitrogen compounds (200-280 ºC) and the relative amount of benzenes (280-300 ºC) and decreases the relative amounts of alkanes, ketones and phenols. Increasing the reaction time weakens the effect of the pressure, and this same pressure increase leads to increases in the proportion of nitrogen derived species (200-250 ºC) and benzenes and alkanes (250-300 ºC) together with decreases in the

relative amounts of ketones, phenols and furans. Nevertheless, these developments are not practically important.

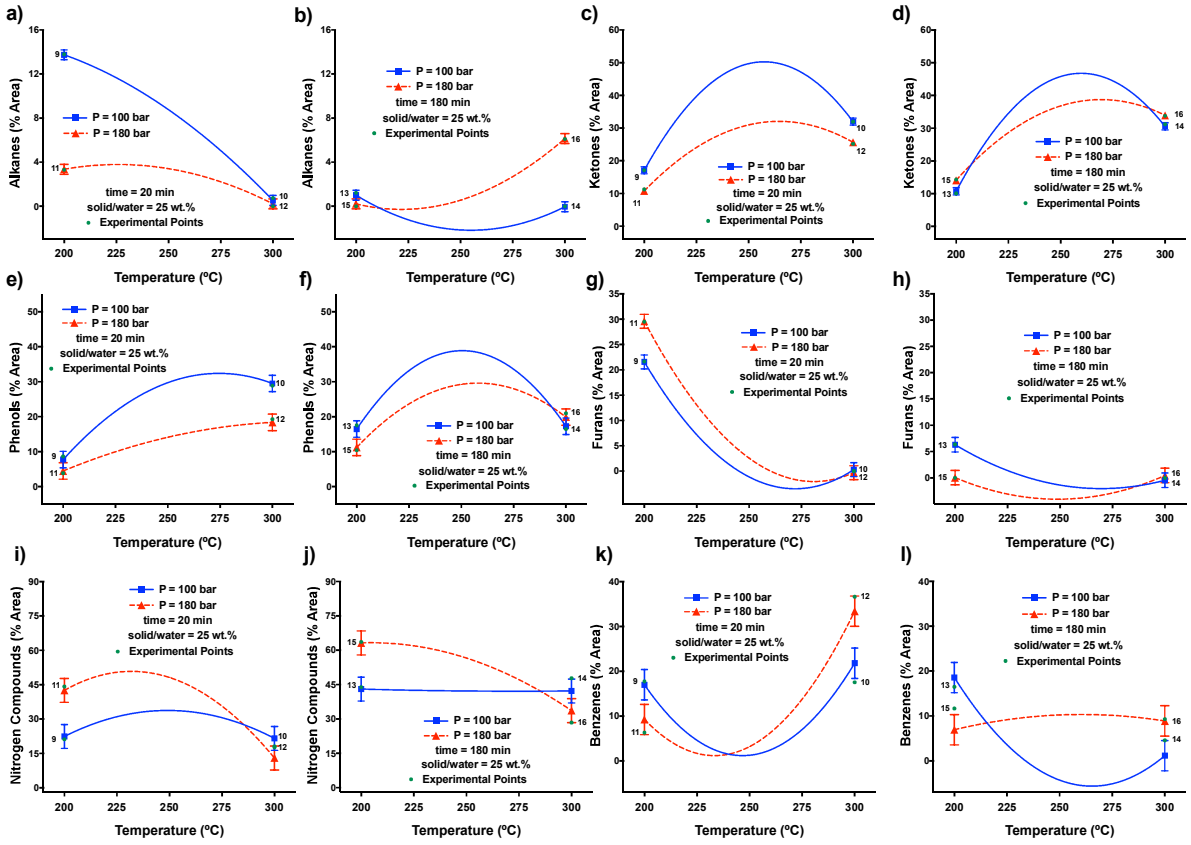

Figure 9. Interaction plots showing the effects of the processing conditions on the chemical composition of the bio-oil using a solid/water ratio of 25 wt.%. Error bars display 95% confidence intervals.

3.2.5 Elemental composition and HHV of the hydro-char

The solid product obtained from the HTT of almond hulls resembles a hydro-char like solid material whose relative amounts of C, H, O and N and HHV vary as follows: 54-74 wt.%, 5-6 wt.%, 1-3 wt.% and 21-31 MJ/kg. The operating conditions exert a significant influence on the elemental composition and HHV of the solid product. The complete influence of the conditions determined by the cause-effect Pareto test (Table S2) is included as supplementary information. These influences fall into the line of previous work reporting on the influence of processing conditions on the elemental composition of hydro-chars produced from biomass (Afolabi et al., 2020; Saqib et al., 2019). Figure 10 a/e/i/m/q and b/f/j/n/r show the effects of the temperature at 100 and 180 bar for a reaction time of 20 and 180 min on the relative amounts of C/H/O/N/and HHV of the hydro-char, using a solid loading of 5 wt.%. These effects are plot in Figure 10 c/g/k/o/s and d/h/l/p/t for a solid loading of 25 wt.%.

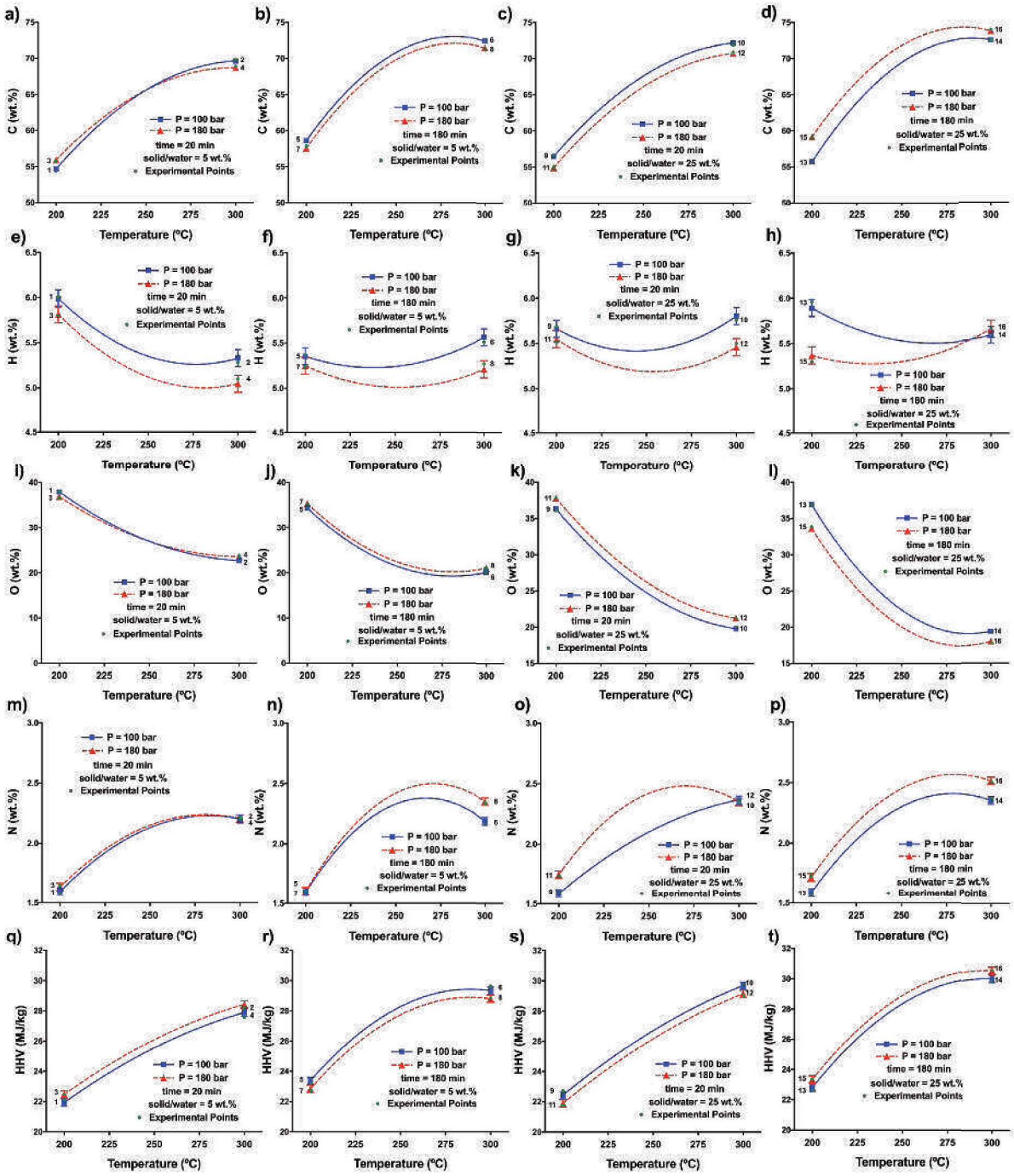

Figure 10. Interaction plots showing the effects of the processing conditions on the elemental composition and HHV of the hydro-char. Error bars display 95% confidence intervals.

The elemental composition and HHV of the hydro-char primary depend on the reaction temperature, the effects of the other conditions being much weaker. In particular, variations in the temperature mostly change the proportions of C and O in the solid, while the relative amounts of H and N are less affected. The proportions of H and N in the hydro-char are relatively low and the variations observed are mostly influenced by the temperature and pressure. In general, irrespective of the other conditions, increasing the temperature leads to small decreases in the proportion of H along with minor increases (between 200

691 and 270 ºC) in the relative amount of N. An upturn in the pressure between 100 and 180 bar leads to a
692 soft decrease in the proportion of H and a minor increase in the relative amount of N. Irrespective of the
693 other operating conditions, an increase in the temperature leads to an increase in the relative amount of C
694 and a depletion in the proportion of O in the solid, which results in an enhancement of the HHV of the
695 solid product. These variations are particularly marked between 200 and 275 ºC, while a steady evolution
696 takes place between 275 and 300 ºC. These changes are the result of the beneficial impact of the
697 temperature on deoxygenation, dehydration and decarboxylation reactions (Duan et al., 2013; Duan and
698 Savage, 2011a; Duan and Savage, 2011b; Fisk et al., 2009). Specifically, these developments increase
699 the proportions of C and H at the expenses of the concentrations of O and N in the hydro-char. The
700 levelling off taking place between 275-300 ºC might be the outcome of the opposition of two different
701 developments: cracking and pyrolysis reactions, favouring deoxygenation, against condensation,
702 crystallisation and re-polymerisation, augmenting the production of hydro-char (Dimitriadis and
703 Bezergianni, 2017; Xu and Lancaster, 2008). Besides, increasing the reaction temperature leads to a
704 decrease in the volatile matter along with an increase in the fixed carbon content of the hydro-char, thus
705 improving the fuel properties of the material (Saqib et al., 2019).
706
707 The influence of the reaction time depends on the solid/water ratio and pressure. For a diluted suspension
708 (5 wt.%), irrespective of the pressure, prolonging the reaction time upsurges the relative amount of C and
709 decreases the proportion of O in the solid, thus increasing the HHV of the bio-char due to the positive
710 kinetic effect of the reaction time on deoxygenation, decarboxylation, dehydration and thermal cracking
711 reactions (Duan et al., 2013; Duan and Savage, 2011a; Duan and Savage, 2011b; Fisk et al., 2009).
712 Conversely, for a solid/water ratio of 25 wt.% the effect of the reaction time depends on the pressure. For
713 a low pressure (100 bar), increasing the reaction time does not markedly alter the relative amounts of C
714 and O in the hydro-char. The antagonism between cracking and pyrolysis reactions against condensation,
715 crystallisation and re-polymerisation reactions, these latter increasing char formation (Dimitriadis and
716 Bezergianni, 2017; Xu and Lancaster, 2008), might be responsible for the levelling off taking place for
717 the relative amounts of C and O in the hydro-char. This is in line with the minimal variations occurring
718 for the solid yield when the reaction time increases from 20 to 180 min as described above. Contrariwise,
719 for a high pressure (180 bar), this same time upsurges the proportion of C at the expenses of the relative

amount of O, which enhances the HHV of the solid. The substantial decrease observed in the solid yield, described above, due to the positive kinetic effect of the pressure on the process, which promotes the impact of the reaction time, might be responsible for such variations. This positive pressure effect makes it possible that deoxygenation, decarboxylation, dehydration and thermal cracking reactions occur to a more substantial extent. This increases and decreases the proportion of C and O in the hydro-char, respectively. As a result of these variations, the effect of the pressure is only significant when using a concentrated suspension, with two different developments taking place depending on the reaction time. On the one hand, for a short reaction time, an increase in the pressure from 100 to 180 bar diminishes the proportion of C and upsurges the relative amount of O, thus depleting the HHV of the solid. On the other, the opposite effect is observed when using a reaction time of 180 min, i.e., the proportion of C and the HHV of the solid increase, while the relative amount of O in the solid decreases.

3.2.6 Chemical composition of the aqueous phase

The aqueous product obtained from the liquid effluent after bio-oil extraction is made up of a mixture of oligosaccharides (55-92 C-wt.%), saccharides (1-7 C-wt.%), carboxylic acids (6-43 C-wt.%), ketones (0-1 C-wt.%) and furans (1-5 C-wt.%). The detailed chemical composition is provided as supplementary material in Table S4. The complete influence of the conditions determined by the cause-effect Pareto test (Table S2) is included as supplementary information. Figure 11 shows the effects of the temperature at 100 and 180 bar for a reaction time of 20 and 180 min on the chemical composition of the aqueous phase for a solid loading of 5 wt.%. These effects are plot in Figure 12 for a solid loading of 25 wt.%.

The impact of the temperature on the liquid effluent chemical composition depends on the solid/water ratio. For a low solid/water ratio (5 wt.%), different developments take place depending on the total pressure (Figure 11). At low pressure (100 bar), irrespective of the temperature or reaction time, the aqueous phase primarily consists of oligosaccharides with a smaller proportion of carboxylic acids, the relative amounts of other species in the liquid product being deficient and practically unaffected by the operating conditions. These results indicate that for a quick treatment at low pressure, the liquid phase primarily consists of oligomers produced via hydrolysis and depolymerisation of almond hulls, with the other liquid species being recovered in the bio-oil. However, the pressure exerts a significant influence

on the composition of the aqueous product, with more essential variations occurring at low than at high temperature. In particular, between 200 and 250 ºC increasing the pressure from 100 to 180 bar leads to a substantial decrease in the proportion of oligosaccharides along with an increase in the relative amount of carboxylic acids, as the positive kinetic effect of the pressure promotes the gradual conversion of the former into the latter species by hydrolysis reactions. Besides, at 180 bar, increasing the temperature between 200 and 300 ºC leads to a substantial increase and decrease in the proportions of oligosaccharides and carboxylic acids, respectively. At high pressure, increasing the reaction time leads to a considerable increase in gas production, which favours the transformation of light oxygenates into gaseous products, thus augmenting the concentration of oligosaccharides in the aqueous effluent. As a result of these developments, the effect of the pressure is very weak between 250 and 300 ºC. Unrelatedly of the pressure, prolonging the reaction time from 20 to 180 min upsurges the relative amount of oligosaccharides at the expenses of the proportion of carboxylic acids due to the higher gas formation at these conditions.

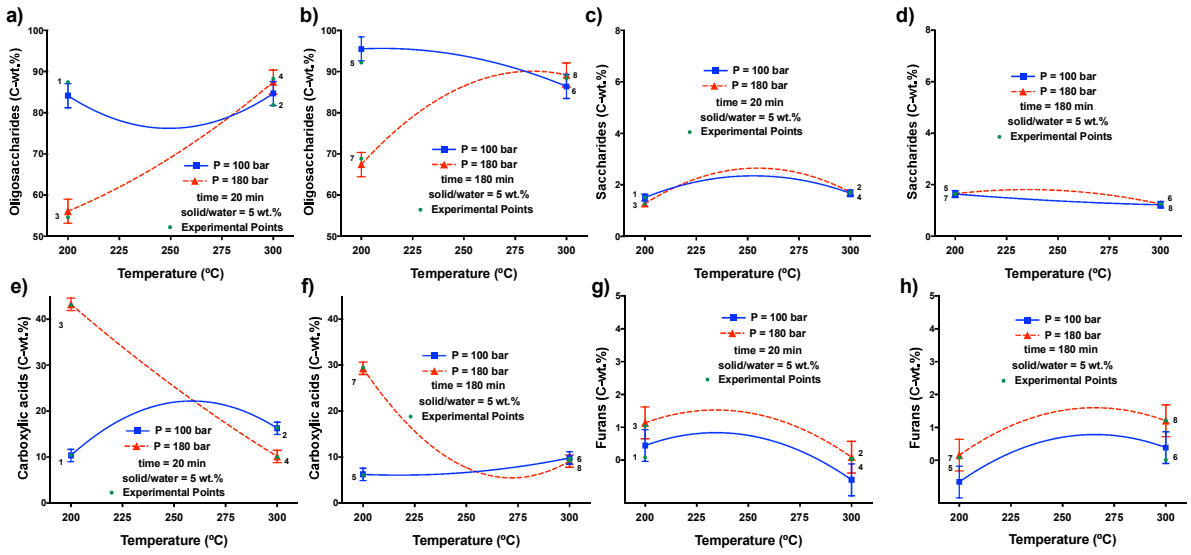

Figure 11. Interaction plots showing the effects of the processing conditions on the chemical composition of the aqueous phase using a solid/water ratio of 5 wt.%. Error bars display 95% confidence intervals.

Increasing the solid/water ratio decreases the relative amount of oligosaccharides and increases the proportion of saccharides in the aqueous product (Figure 11 vs Figure 12). This solid loading increase also augments the proportion of carboxylic acids (especially at low pressure and high temperature), and furans, in some cases. Besides, the effects of the temperature on the composition of the aqueous product

weaken as the solid water/ratio increases. As a result, for a solid/water ratio of 25 wt.% (Figure 12), the chemical composition of the liquid phase is not strongly influenced by the temperature. On the one hand, for a short reaction time (20 min), more critical variations for the composition of the aqueous product take place at low than at high pressure. In particular, at 100 bar, an initial temperature increment from 200 to 270 ºC upsurges the concentrations of saccharides and carboxylic acids and diminishes the proportions of oligosaccharides and furans in the aqueous phase. Increasing the temperature promotes a more important shift of hydrolysis and depolymerisation reactions, which allows the transformation of oligosaccharides into saccharides as well as the subsequent degradation of these species into secondary products, i.e., carboxylic acids and furans augmenting the total pressure from 100 to 180 bar increases the proportion of oligosaccharides and furans and decreases the concentrations of saccharides and carboxylic acids. Besides the higher the temperature, the weaker is the effect of the pressure on the chemical composition of the aqueous product. This is believed to account for the decrease occurring in the solid yield when the pressure increases when a concentrated suspension is used for a short reaction time, as described earlier. As a result, at 180 bar, the chemical composition is barely affected by the reaction temperature.

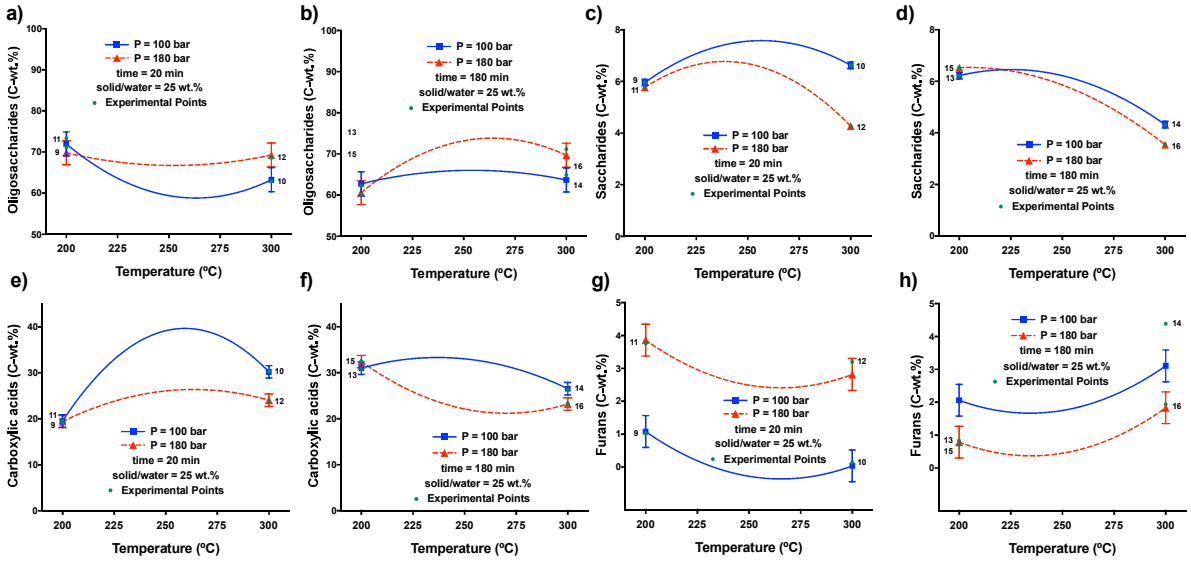

Figure 12. Interaction plots showing the effects of the processing conditions on the chemical composition of the aqueous phase using a solid/water ratio of 25 wt.%. Error bars display 95% confidence intervals.

On the other hand, for a long reaction time (180 min), a similar liquid composition is achieved than that described for a short reaction time (20 min) as the reaction time influence on the composition of the

aqueous effluent for a high solid loading is relatively low. Also, different temperature evolutions take place depending on the pressure. At low pressure (100 bar), the chemical composition is barely affected by the temperature, and only minimal variations take place for the proportions of saccharides and furans. However, these are not practically important as the liquid largely consists of a mixture of oligosaccharides and carboxylic acids, which indicates that other oxygenated compounds were extracted in the bio-oil during the liquid-liquid separation. Increasing the pressure from 100 to 180 bar leads to an increase in the proportion of oligosaccharides and a diminution in the proportion of carboxylic acids, probably due to the rise occurring in the liquid yield as described above. Besides, at 180 bar, increasing the temperature from 200 to 250 ºC results in a soft increase in the proportion of oligosaccharides at the expenses of the relative amount of carboxylic acids due to favourable temperature kinetic influence on biomass conversion, which promotes biomass depolymerisation, thus raising the proportion of oligosaccharides as oligosaccharides formation might be faster than its decomposition, thus increasing their proportion in the aqueous product.

3.3 Theoretical optimisation and energy assessment

Five addressable optimisation scenarios were sought using the empirical statistical formulae developed from the ANOVA analyses. Optimisations 1-3 are directed towards the production of liquid and solid biofuels, while Optimisations 4 and 5 comprise the production of value-added liquids. In particular, Opt. 1 and 2 consider the individual production of high energy bio-oil (bio-crude) and hydro-char, respectively, by maximising the product (bio-oil or hydro-char) yields and their corresponding HHV. Besides, Opt. 3 investigates the simultaneous transformation of almond hulls into energy-dense biofuels (bio-oil and hydro-char). Therefore, the yields to bio-oil and hydro-char and their HHVs have been maximised. Opt. 4 includes the production of renewable-based antioxidants via the production of a bio-oil with a high proportion of phenolic compounds. Opt. 5 is directed towards the production of aqueous sugar-rich carriers by maximising the aqueous yield together with the relative amounts of oligosaccharides and saccharides in this product. To come up with solutions that satisfy all these criteria, a relative importance (from 1 to 5) has been given to each constraint. Table 3 list the optimisation restraints and the optimisation results for each optimum.

822 **Table 3. Optimisation. Restrictions and optimum conditions.**

Optimisation	1		2		3		4		5	
	Obj.	Solution	Obj.	Solution	Obj.	Solution	Obj.	Solution	Obj.	Solution
Temperature (ºC)		250		270		256		250		252
Pressure (bar)		128		100		100		144		180
time (min)		150		180		157		167		153
Solid/water (wt.%)		5		25		5		5		24
Global results										
Gas yield (%)		2.92±0.65		9.58±0.65		2.83±0.65		3.45±0.65		8.56±0.65
Solid yield (%)		33.57±0.14	Max (3)	39.48±0.14	Max (3)	32.12±0.14		34.50±0.14		38.26±0.14
Bio-oil yield (%)	Max (3)	11.02±0.34		1.22±0.34	Max (3)	10.50±0.34	Max (3)	10.13±0.34		1.35±0.34
Aqueous yield (%)		51.91±1.07		49.99±1.07		52.56±1.07		51.87±1.07	Max (3)	54.18±1.07
Gas composition and LHV										
H_2 (vol.%)		13.58±0.47		0±0.47		10.14±0.47		12.80±0.47		0±0.47
CO_2 (vol.%)		42.27±2.75		91.91±2.75		56.18±2.75		46.54±2.75		90.01±2.75
CO (vol.%)		21.45±2.54		8.82±2.54		18.52±2.54		25.59±2.54		9.09±2.54
CH_4 (vol.%)		15.62±1.08		0±1.08		10.51±1.08		13.23±1.08		0±1.08
LHV (MJ/m³ STP)		10.53±0.95		2.57±0.95		8.79±0.95		10.73±0.95		0.96±0.95
Bio-oil elemental composition and HHV										
C (wt.%)		64.28±1.71		46.19±1.71		63.30±1.71		65.41±1.71		61.63±1.71
H (wt.%)		7.38±0.34		7.27±0.34		7.32±0.34		7.49±0.34		7.61±0.34
O (wt.%)		23.86±2.76		42.03±2.76		22.63±2.76		23.43±2.76		26.71±2.76
N (wt.%)		3.11±0.53		1.74±0.53		3.48±0.53		2.97±0.53		2.85±0.53
HHV (MJ/kg)	Max (5)	29.10±1.02		20.73±1.02	Max (5)	29.31±1.02		29.50±1.02		28.4±1.02
Solid elemental composition and HHV										
C (wt.%)		64.28±0.29		72.05±0.29		71.27±0.29		70.08±0.29		71.31±0.29
H (wt.%)		7.38±0.08		5.50±0.08		5.27±0.08		5.30±0.08		5.26±0.08
O (wt.%)		23.86±0.27		19.73±0.27		20.99±0.27		22.18±0.27		20.62±0.27
S (wt.%)		0.001±0.03		0.04±0.03		0.06±0.03		0.00±0.03		0.00±0.03
N (wt.%)		3.11±0.02		2.40±0.02		3.47±0.02		2.33±0.02		2.45±0.02
HHV (MJ/kg)		29.07±0.32	Max (5)	29.53±0.32	Max (5)	29.32±0.32		28.01±0.32		28.91±0.32
Bio-oil chemical Composition (Area %)										
Ketones		30.99±0.90		45.49±0.90		42.95±0.90	Min (5)	33.66±0.90		30.82±0.90
Phenols		40.51±1.72		35.19±1.72		36.46±1.72	Max (5)	44.52±1.72		27.12±1.72
Alcohols		0±0.29		1.54±0.29		0±0.29	Min (5)	0±0.29		2.25±0.29
Furans		3.20±0.96		0±0.96		1.14±0.96	Min (5)	3.10±0.96		0±0.96
Cyclic Compounds		1.17±0.00		0.07±0.00		1.22±0.00	Min (5)	1.13±0.00		0.17±0.00
Nitrogen Compounds		18.80±5.42		42.08±5.42		27.09±5.42	Min (5)	14.44±5.42		51.88±5.42
Benzenes		7.82±3.20		0±3.20		2.27±3.20	Min (5)	5.47±3.20		0±3.20
Aqueous Liquid phase chemical Composition (C-wt. %)										
Oligosaccharides		89.74±2.54		65.71±2.54		92.19±2.54		89.26±2.54	Max (5)	74.79±2.54
Saccharides		1.40±0.08		5.25±0.08		1.48±0.08		1.35±0.08	Max (5)	5.81±0.08
C. Acids		7.62±0.84		31.36±0.84		7.13±0.84		7.45±0.84	Min (5)	19.56±0.84
Furans		0.32±0.58		2.10±0.58		0.74±0.58		0.42±0.58	Min (5)	0.87±0.58
Energy Efficiency										
E (%)		83.97		76.49		84.49		80.83		73.03

823

824 Opt. 1 shows that using a temperature of 250 ºC and a pressure of 128 bar with a solid/water ratio of 5
825 wt.% for 150 min, it is possible to transform up to 11% of almond hulls into a high energy (29 MJ/kg)
826 bio-oil. Opt. 2 reveals that operating at a temperature of 270 ºC with a pressure of 100 bar and a solid
827 loading of 25 wt.% for 180 min permits the transformation of 40% of the feedstock into a solid product,
828 resembling a hydro-char like material with a HHV of 30 MJ/kg. Also, at 256 ºC, 100 bar and using a 5
829 wt.% solid loading for a 157 min (Opt. 3), it is possible to simultaneously convert 43% of the almond
830 hulls into a high energy dense bio-oil (11% yield, 30 MJ/kg) and a high energetic hydro-char (32% yield,
831 29 MJ/kg). The calorific values of bio-oils and hydro-chars obtained at optimum conditions are twice as

high as that of the original feedstock (15 MJ/kg) and similar to the highest HHV reported by other authors during the hydrothermal treatment of different types of biomass (26-34 MJ/kg) (Saqib et al., 2019; Yang et al., 2019); thus clearly highlighting the potential of HTT of almond hulls for energy applications. On the one hand, the bio-oil has akin fuel characteristics than diesel (C = 85 wt.%, H = 15 wt.%, 44 MJ/kg) and biodiesel (C=75 wt.%, H =12 wt.%, O= 11 wt.%, 40 MJ/kg) (Prakash et al., 2013) which make it suitable to be combusted in current engines, either alone and/or blended (Cataluña et al., 2013). On the other, the hydro-char HHV falls between lignite (29 MJ/kg) and coke (33 MJ/kg) (Li et al., 2017).

Regarding value-added liquid products, Opt. 4 shows that it is possible to convert up to 10% of the almond hulls into a bio-oil with a high proportion (45%) of phenolic compounds when a temperature of 250 ºC is used at a pressure of 144 bar with a solid loading of 5 wt.% for 167 min. This bio-oil not only might be an excellent starting material for the sustainable production of aromatic compounds but also its high aromaticity converts this liquid product into a superb precursor for the production of biofuels and/or renewable-based liquid fuel additives to enhance the oxidation stability of other fuels. Liquid-liquid extraction and/or vacuum distillation can be used in the selective separation of these species. Besides, there are several studies in the literature that blend biodiesel with bio-oil, resulting in the spontaneous solubilisation of phenolic compounds into the biodiesel which leads to an increase in the oxidation stability of the biofuel (Pinheiro Pires et al., 2019). Besides, Opt. 5 reveals that 54% of the original feedstock can be transformed into a sugar (oligo- and saccharides) rich (81 C-wt.%) aqueous solution, which might serve as natural prebiotic compounds, by treating a 24 wt.% almond hull suspension at 252ºC and 180 bar for 153 min. Carboxylic acids and furans can be removed from this sugar-rich solution by vacuum distillation and/or liquid-liquid extraction (Remón et al., 2018a). Run 14 was conducted using operating conditions (T = 300 ºC, P= 100 bar, t = 180 min and solid/water ratio = 25%) very close to the optimum predicted in Opt. 2 and very similar results were experimentally obtained, which can prove validation for the theoretical predictions gathered making use of the experimental models developed with the ANOVA analysis in the optimisation process. For all these optima, energy assessments, based on the energy of the products with respect to the calorific value of the original feedstock (Table 1), were conducted. Table 3 reveals that energy efficiencies between 73 and 85% were attained for all the scenarios considered. Amongst the different case scenarios considered, Opt. 3, with an energy efficiency of 85% is

probably the most economically efficient solution. It allows the simultaneous conversion and of almond hulls into energy-dense (30 MJ/kg), marketable liquid and solid biofuels (bio-oil and hydro-char) along with a sugar rich-solution containing a high proportion (90 C-wt.%) of oligosaccharides that could be used as natural prebiotic compounds (Remón et al., 2019a). However, fluctuations in the energy and chemical markets might take place during the industrial implementation of this technology, and, therefore, this assumption must be continuously re-evaluated. Therefore, these promising results are a step-change in future energy and chemicals production, not only aiding to render the entire biorefinery for almond hulls more cost-effectively and environmentally viable, but also providing innovative insights into the development of alternative and ecologically sustainable routes for biomass valorisation.

4. Conclusions

This work addresses a novel biorefinery concept for the simultaneous conversion of almond hulls into biofuels and value-added chemicals by hydrothermal treatment (HTT), examining the influences of the processing parameters on the process. The most relevant conclusions are recapped as follows.

1. The HTT of almond hulls allowed the transformation of almond hulls into gas, bio-oil, aqueous fraction and hydro-char with variable yields (2-13%, 2-12%, 4-69% and 17-89%, respectively), depending on the operating conditions. High temperatures and pressures combined with prolonged reaction times favoured gas production regardless of the solid loading, while high bio-oil yields were attained using low solid/water ratios and short reaction times. An increase in the temperature decreased hydro-char formation and increased the formation of aqueous liquids products.

2. The gas-phase comprised a mixture of H_2, CO_2, CO and CH_4 with a LHV shifting between 1 and 13 MJ/m^3 STP. The gas composition primary depended on the extension of decarboxylation reactions, as these promote CO_2 formation, and the thermodynamics of the water-gas shift and methane reforming reactions. The aqueous phase was made up of a mixture of oligosaccharides and saccharides together with small oxygenates such as carboxylic acids and furans. Oligosaccharides were the most abundant species at low temperatures and short reaction times. Increasing the temperature, pressure or reaction time resulted in the first decomposition of oligosaccharides into carboxylic acids and furans, followed by a subsequent decomposition of these species into gaseous products.

3. The bio-oil was largely made up of a mixture of alkanes, aldehydes, ketones, phenols, furans, benzenes and nitrogen compounds, with variable amounts of C (57-74 wt.%), H (5-6 wt.%), O (18-38 wt.%) and N (1-3 wt.%) and HHV between 21 and 31 MJ/kg. The solid product resembled a hydro-char like solid material whose relative amounts of C, H, O and N and HHV varied as follows: 54-74 wt.%, 5-6 wt.%, 1-3 wt.% and 21-31 MJ/kg. Increasing the temperature, pressure and time promoted a greater spread of deoxygenation, carbonisation, dehydration and thermal cracking reactions which increased the HHV of both products.

4. Process optimisation revealed that it is possible to transform almond hulls into bio-fuels and/or platform chemicals with high energy efficiencies (73-85%). At 256 ºC, 100 bar, using a 5 wt.% solid loading for a 157 min, 43% of the almond hulls can be converted into a high energy dense bio-oil (11% yield, 30 MJ/kg) together with a high energetic hydro-char (32% yield, 29 MJ/kg), calorific values twice as high as that of the original feedstock (15 MJ/kg). Besides, 10% of the original material can be converted into a bio-oil with a high proportion (45%) of phenolic compounds at 250 ºC and 144 bar with a solid loading of 5 wt.% for 167 min. Also, 54% of this material can be transformed into a sugar-rich (81 C-wt.%) aqueous effluent by treating a 24 wt.% suspension at 252ºC and 180 bar for 153 min.

5. The 'almond-refinery' concept developed in this work exemplifies a landmark achievement in future energy and chemicals production from biomass, which might help render the complete bio-refinery for almond hulls more cost-effectively and ecologically feasible. However, more work is still necessary to gain the full potential of this technology. Future research might be directed towards the development of heterogeneous catalysts for the process and/or the use of alternative autocatalytic reaction media or synergistic co-valorisation strategies.

Acknowledgements

The authors wish to express their gratefulness to FEDER and the Ministerio de Ciencia, Innovación y Universidades (Grant Number ENE2017-83854-R) for providing financial support. Besides, Javier Remón Núñez is very grateful to the Ministerio de Ciencia, Innovación y Universidades for the Juan de la Cierva (JdC) fellowships (Grant Numbers FJCI-2016-30847 and IJC2018-037110-I) awarded.

References

http://www.factfish.com/statistic/almonds%2C%20production%20quantity, April 2020a.

https://www.driedfruit.net/world-almond-production-kernel-basis-metric-tons.html, April 2020b.

Afolabi OOD, Sohail M, Cheng Y-L. Optimisation and characterisation of hydrochar production from spent coffee grounds by hydrothermal carbonisation. Renewable Energy 2020; 147: 1380-1391.

Aktas T, Thy P, Williams RB, McCaffrey Z, Khatami R, Jenkins BM. Characterization of almond processing residues from the Central Valley of California for thermal conversion. Fuel Processing Technology 2015; 140: 132-147.

Arturi KR, Kucheryavskiy S, Søgaard EG. Performance of hydrothermal liquefaction (HTL) of biomass by multivariate data analysis. Fuel Processing Technology 2016; 150: 94-103.

Attard TM, Clark JH, McElroy CR. Recent developments in key biorefinery areas. Current Opinion in Green and Sustainable Chemistry 2020; 21: 64-74.

Cataluña R, Kuamoto PM, Petzhold CL, Caramão EB, Machado ME, da Silva R. Using Bio-oil Produced by Biomass Pyrolysis as Diesel Fuel. Energy & Fuels 2013; 27: 6831-6838.

Channiwala SA, Parikh PP. A unified correlation for estimating HHV of solid, liquid and gaseous fuels. Fuel 2002; 81: 1051-1063.

Clark JH. Green biorefinery technologies based on waste biomass. Green Chemistry 2019; 21: 1168-1170.

Dimitriadis A, Bezergianni S. Hydrothermal liquefaction of various biomass and waste feedstocks for biocrude production: A state of the art review. Renewable and Sustainable Energy Reviews 2017; 68: 113-125.

Duan P, Bai X, Xu Y, Zhang A, Wang F, Zhang L, et al. Catalytic upgrading of crude algal oil using platinum/gamma alumina in supercritical water. Fuel 2013; 109: 225-233.

Duan P, Savage PE. Catalytic hydrotreatment of crude algal bio-oil in supercritical water. Applied Catalysis B: Environmental 2011a; 104: 136-143.

Duan P, Savage PE. Catalytic treatment of crude algal bio-oil in supercritical water: optimization studies. Energy & Environmental Science 2011b; 4: 1447.

Egües I, Alriols MG, Herseczki Z, Marton G, Labidi J. Hemicelluloses obtaining from rapeseed cake residue generated in the biodiesel production process. Journal of Industrial and Engineering Chemistry 2010; 16: 293-298.

Elliott DC, Biller P, Ross AB, Schmidt AJ, Jones SB. Hydrothermal liquefaction of biomass: developments from batch to continuous process. Bioresour Technol 2015a; 178: 147-56.

Elliott DC, Biller P, Ross AB, Schmidt AJ, Jones SB. Hydrothermal liquefaction of biomass: Developments from batch to continuous process. Bioresource Technology 2015b; 178: 147-156.

Esfahlan AJ, Jamei R, Esfahlan RJ. The importance of almond (Prunus amygdalus L.) and its by-products. Food Chemistry 2010; 120: 349-360.

Ferrandez-Villena M, Ferrandez-Garcia CE, Garcia Ortuño T, Ferrandez-Garcia A, Ferrandez-Garcia MT. Study of the Utilisation of Almond Residues for Low-Cost Panels. Agronomy 2019; 9.

Fisk CA, Morgan T, Ji Y, Crocker M, Crofcheck C, Lewis SA. Bio-oil upgrading over platinum catalysts using in situ generated hydrogen. Applied Catalysis A: General 2009; 358: 150-156.

Gollakota ARK, Kishore N, Gu S. A review on hydrothermal liquefaction of biomass. Renewable and Sustainable Energy Reviews 2018; 81: 1378-1392.

González JF, González-García CM, Ramiro A, Gañán J, González J, Sabio E, et al. Use of almond residues for domestic heating. Study of the combustion parameters in a mural boiler. Fuel Processing Technology 2005; 86: 1351-1368.

Hu L, Luo Y, Cai B, Li J, Tong D, Hu C. The degradation of the lignin in Phyllostachys heterocycla cv. pubescens in an ethanol solvothermal system. Green Chemistry 2014; 16: 3107-3116.

Kahlaoui M, Borotto Dalla Vecchia S, Giovine F, Ben Haj Kbaier H, Bouzouita N, Barbosa Pereira L, et al. Characterization of Polyphenolic Compounds Extracted from Different Varieties of Almond Hulls (Prunus dulcis L.). Antioxidants (Basel) 2019; 8.

Kumar M, Olajire Oyedun A, Kumar A. A review on the current status of various hydrothermal technologies on biomass feedstock. Renewable and Sustainable Energy Reviews 2018; 81: 1742-1770.

Li T, Remón J, Shuttleworth PS, Jiang Z, Fan J, Clark JH, et al. Controllable production of liquid and solid biofuels by doping-free, microwave-assisted, pressurised pyrolysis of hemicellulose. Energy Conversion and Management 2017; 144: 104-113.

975 Lorente A, Remón J, Budarin VL, Sánchez-Verdú P, Moreno A, Clark JH. Analysis and optimisation of
976 a novel "bio-brewery" approach: Production of bio-fuels and bio-chemicals by microwave-
977 assisted, hydrothermal liquefaction of brewers' spent grains. Energy Conversion and
978 Management 2019; 185: 410-430.
979 Meneses NGT, Martins S, Teixeira JA, Mussatto SI. Influence of extraction solvents on the recovery of
980 antioxidant phenolic compounds from brewer's spent grains. Separation and Purification
981 Technology 2013; 108: 152-158.
982 Muppaneni T, Reddy HK, Selvaratnam T, Dandamudi KPR, Dungan B, Nirmalakhandan N, et al.
983 Hydrothermal liquefaction of Cyanidioschyzon merolae and the influence of catalysts on
984 products. Bioresource Technology 2017; 223: 91-97.
985 Ochoa E, Torres D, Moreira R, Pinilla JL, Suelves I. Carbon nanofiber supported Mo2C catalysts for
986 hydrodeoxygenation of guaiacol: The importance of the carburization process. Applied Catalysis
987 B: Environmental 2018; 239: 463-474.
988 Ochoa E, Torres D, Pinilla JL, Suelves I. Influence of carburization time on the activity of Mo2C/CNF
989 catalysts for the HDO of guaiacol. Catalysis Today 2019.
990 Offeman RD, Dao GT, Holtman KM, Orts WJ. Leaching behavior of water-soluble carbohydrates from
991 almond hulls. Industrial Crops and Products 2015; 65: 488-495.
992 Offeman RD, Holtman KM, Covello KM, Orts WJ. Almond hulls as a biofuels feedstock: Variations in
993 carbohydrates by variety and location in California. Industrial Crops and Products 2014; 54: 109-
994 114.
995 Pinelo M, Rubilar M, Sineiro J, Núñez MJ. Extraction of antioxidant phenolics from almond hulls (
996 Prunus amygdalus) and pine sawdust (Pinus pinaster). Food Chemistry 2004; 85: 267-273.
997 Pinheiro Pires AP, Arauzo J, Fonts I, Domine ME, Fernández Arroyo A, Garcia-Perez ME, et al.
998 Challenges and Opportunities for Bio-oil Refining: A Review. Energy & Fuels 2019; 33: 4683-
999 4720.
1000 Pińkowska H, Wolak P, Oliveros E. Hydrothermolysis of rapeseed cake in subcritical water. Effect of
1001 reaction temperature and holding time on product composition. Biomass and Bioenergy 2014;
1002 64: 50-61.
1003 Prakash R, Singh RK, Murugan S. Experimental investigation on a diesel engine fueled with bio-oil
1004 derived from waste wood–biodiesel emulsions. Energy 2013; 55: 610-618.
1005 Remón J, Jarauta-Córdoba C, García L, Arauzo J. Analysis and optimisation of H2 production from crude
1006 glycerol by steam reforming using a novel two step process. Fuel Processing Technology 2016a;
1007 145: 130-147.
1008 Remón J, Laseca M, García L, Arauzo J. Hydrogen production from cheese whey by catalytic steam
1009 reforming: Preliminary study using lactose as a model compound. Energy Conversion and
1010 Management 2016b; 114: 122-141.
1011 Remón J, Li T, Chuck CJ, Matharu AS, Clark JH. Toward Renewable-Based, Food-Applicable Prebiotics
1012 from Biomass: A One-Step, Additive-Free, Microwave-Assisted Hydrothermal Process for the
1013 Production of High Purity Xylo-oligosaccharides from Beech Wood Hemicellulose. ACS
1014 Sustainable Chemistry & Engineering 2019a; 7: 16160-16172.
1015 Remón J, Matharu AS, Clark JH. Simultaneous production of lignin and polysaccharide rich aqueous
1016 solutions by microwave-assisted hydrothermal treatment of rapeseed meal. Energy Conversion
1017 and Management 2018a; 165: 634-648.
1018 Remón J, Mercado V, García L, Arauzo J. Effect of acetic acid, methanol and potassium hydroxide on
1019 the catalytic steam reforming of glycerol: Thermodynamic and experimental study. Fuel
1020 Processing Technology 2015; 138: 325-336.
1021 Remón J, Ochoa E, Foguet C, Pinilla JL, Suelves I. Towards a sustainable bio-fuels production from
1022 lignocellulosic bio-oils: Influence of operating conditions on the hydrodeoxygenation of guaiacol
1023 over a Mo2C/CNF catalyst. Fuel Processing Technology 2019b; 191: 111-120.
1024 Remón J, Randall J, Budarin VL, Clark JH. Production of bio-fuels and chemicals by microwave-assisted,
1025 catalytic, hydrothermal liquefaction (MAC-HTL) of a mixture of pine and spruce biomass. Green
1026 Chemistry 2019c; 21: 284-299.
1027 Remón J, Santomauro F, Chuck CJ, Matharu AS, Clark JH. Production of fermentable species by
1028 microwave-assisted hydrothermal treatment of biomass carbohydrates: reactivity and
1029 fermentability assessments. Green Chemistry 2018b; 20: 4507-4520.
1030 Ren S, Ye XP, Borole AP. Separation of chemical groups from bio-oil water-extract via sequential
1031 organic solvent extraction. Journal of Analytical and Applied Pyrolysis 2017; 123: 30-39.

Saqib NU, Sharma HB, Baroutian S, Dubey B, Sarmah AK. Valorisation of food waste via hydrothermal carbonisation and techno-economic feasibility assessment. Sci Total Environ 2019; 690: 261-276.
Schienbein P, Marx D. Assessing the properties of supercritical water in terms of structural dynamics and electronic polarization effects. Phys Chem Chem Phys 2020; 22: 10462-10479.
Sfahlan AJ, Mahmoodzadeh A, Hasanzadeh A, Heidari R, Jamei R. Antioxidants and antiradicals in almond hull and shell (Amygdalus communis L.) as a function of genotype. Food Chemistry 2009; 115: 529-533.
Thiruvenkadam S, Izhar S, Yoshida H, Danquah MK, Harun R. Process application of Subcritical Water Extraction (SWE) for algal bio-products and biofuels production. Applied Energy 2015; 154: 815-828.
Toor SS, Rosendahl L, Rudolf A. Hydrothermal liquefaction of biomass: A review of subcritical water technologies. Energy 2011; 36: 2328-2342.
Xu C, Lancaster J. Conversion of secondary pulp/paper sludge powder to liquid oil products for energy recovery by direct liquefaction in hot-compressed water. Water Res 2008; 42: 1571-82.
Yang J, He Q, Niu H, Corscadden K, Astatkie T. Hydrothermal liquefaction of biomass model components for product yield prediction and reaction pathways exploration. Applied Energy 2018; 228: 1618-1628.
Yang J, He Q, Yang L. A review on hydrothermal co-liquefaction of biomass. Applied Energy 2019; 250: 926-945.
Yang W, Li X, Li Z, Tong C, Feng L. Understanding low-lipid algae hydrothermal liquefaction characteristics and pathways through hydrothermal liquefaction of algal major components: crude polysaccharides, crude proteins and their binary mixtures. Bioresour Technol 2015; 196: 99-108.